
REVIEWS

Infrared Radiation in the Energetics of the Atmosphere

B. M. Smirnov*

Joint Institute for High Temperatures, Russian Academy of Sciences, Moscow, 125412 Russia

*e-mail: bmsmirnov@gmail.com

Received December 24, 2018; revised February 10, 2019; accepted March 27, 2019

Abstract—A review of the processes in the Earth's atmosphere that affect its energetics is presented. The energetics balance of the Earth and its atmosphere as a whole is considered, and the results of NASA programs for the monitoring of the global temperature and concentration of carbon dioxide and water in the atmosphere are presented. The spectra of the optically active components of the atmosphere in the infrared region are analyzed on the basis of classical methods of molecular spectroscopy. Spectroscopic data from the HITRAN databank facilitate the analysis and lead to a simple scheme whereby the three main greenhouse components—carbon dioxide, water vapor in the form of free water molecules, and a water droplet—create an infrared radiation flux directed toward the Earth's surface. This radiation is created by water molecules in the range of $0\text{--}580\text{ cm}^{-1}$, the atmospheric radiation in the range of $580\text{--}780\text{ cm}^{-1}$ is determined by the molecules of water and carbon dioxide. At frequencies above 780 cm^{-1} , the contribution to atmospheric radiation due to water molecules is approximately 5%, and the other is determined by the emission of water microdroplets, which partially form clouds. According to this model, at the present atmospheric composition, 52% of the radiation flux to the Earth's surface is created by atmospheric water vapor, and 32% is due to microdroplets of water in the atmosphere, which include about 0.4% of atmospheric water and 14% of the radiation flux is determined by carbon dioxide molecules. Doubling the mass of atmospheric carbon dioxide, which will occur in about 120 years at the current rate of growth of atmospheric carbon dioxide, will lead to an increase in the atmospheric radiation flux towards the Earth by 0.7 W/m^2 , and a 10% increase in the atmospheric concentration of water molecules increases this radiation flux by 0.3 W/m^2 . Doubling of the mass of atmospheric carbon dioxide in a real atmosphere leads to an increase in the global temperature of $2.0 \pm 0.3\text{ K}$ in a real atmosphere, according to NASA data analysis. If the concentration of other components does not change, then the change in global temperature will be $0.4 \pm 0.2\text{ K}$, and the contribution to this change due to industrial emissions of carbon dioxide into the atmosphere is 0.02 K .

DOI: 10.1134/S0018151X19040199

TABLE OF CONTENTS

INTRODUCTION

1. Global properties of the Earth's atmosphere
 - 1.1. Standard atmosphere model
 - 1.2. Evolution of global temperature
2. Greenhouse components of the Earth's atmosphere
 - 2.1. Carbon dioxide in the Earth's atmosphere
 - 2.2. Atmospheric water
3. Atmospheric air absorption coefficient
 - 3.1. A simple model of radiation of the Earth's atmosphere
 - 3.2. Emission of Atmospheric CO_2 molecules and H_2O
4. Atmospheric radiative flows towards the Earth
 - 4.1. Features of atmospheric air radiation
 - 4.2. Atmospheric radiative towards the Earth
 - 4.3. Cosmic rays in the atmosphere
 - 4.4. Partial emission of the atmosphere

4.5. Peculiarities of the greenhouse effect in the atmosphere

CONCLUSIONS

REFERENCES

INTRODUCTION

The nature of the greenhouse effect was understood two hundred years ago [1, 2]. In this case, the energy balance of the considered element of the Earth's surface consists mainly of the absorption of solar radiation flux in the visible spectral region and the emission of radiation in the infrared (IR) region. If a partition is placed in the path of outgoing infrared radiation, which partially returns it, the surface temperature will increase.

This principle underlies the greenhouse effect of the Earth, where the Earth's atmosphere plays the role of a partition as a source of IR radiation. Indeed, the energy flux of infrared radiation absorbed by the Earth's surface is approximately twice the solar flux absorbed by the Earth. In the middle of the 19th century, it was established that molecular gases play the

role of the greenhouse component of the Earth's atmosphere [3, 4]. In accordance with the modern understanding of the greenhouse effect, atmospheric radiators are molecules of carbon dioxide and water, as well as the microdroplets of water that make up clouds. The concentration of these components in atmospheric air is low [5].

Analysis of the atmospheric emission and the passage of thermal radiation through it is of interest for various applications. In the sixties, satellite methods were developed to detect submarines and underground energy objects by their thermal radiation, taking into account its distortion during passage through the atmosphere. The degree of resolution of such measurements has significantly increased and makes it possible to record fires on the ground, starting with their formation, as well as other phenomena accompanied by energy release. In terms of atmospheric energy, the contributions of individual greenhouse components to the thermal flux of the atmosphere, as well as the change in these contributions as the concentration of greenhouse components changes, are of interest. The most popular among these tasks is the change in the global temperature of the Earth with a doubling of the carbon dioxide concentration [6].

General approaches to the analysis of atmospheric emissions, as well as models for this problem, were formulated in the middle of the last century and are presented in books in which the thermal radiation of the atmosphere is considered, starting with Goody's 1964 classic [7]. In particular, the temperature of the radiation flux created by the Earth's atmosphere at local thermodynamic equilibrium at each point is characterized by the air temperature at this point, and the total atmospheric radiation flux at a given frequency is obtained via summing of the fluxes from each point with allowance for their absorption along the way.

A characteristic of the thermal radiation of the Earth's atmosphere, which is largely determined by the vibration-rotation transitions of molecules, is associated with a large difference in the emissivity at the centers of the spectral lines and between adjacent lines. In the case of carbon dioxide in atmospheric air, the ratio of the absorption coefficients in the adjacent maximum and minimum is about 40. For a water molecule with an irregular spectrum structure, this ratio is about an order of magnitude higher. Data from the HITRAN databank [8–10] is used to calculate the radiation flux due to molecular components. It contains the absorption and broadening parameters of individual spectral lines. This database includes the general principles of molecular spectroscopy, and its use makes it possible to avoid model approximations. In this case, the information is taken from the branch of the databank created at the Tomsk Institute of Atmosphere [9], which has a filter that allows the selection of the most powerful transitions. Note that the number of such strong transitions is several hun-

dred, while the databank has the parameters of hundreds of thousands of molecular transitions.

At the same time, the interaction of different greenhouse components is significant, since they are simultaneously radiators and absorbers. For example, an increase in the carbon dioxide concentration leads to an increase in the radiative flux produced by carbon dioxide molecules. However, this is almost compensated by the decrease in the radiative flux generated by water molecules. In this case, the increase in the total radiation flux is about an order of magnitude less than the increase in the radiation flux due to carbon dioxide molecules. Experience shows that the most reliable model in this case is the line-by-line model (line-by-line [7]), which requires determination of the radiation flux for each frequency without averaging over the spectrum.

Another problem with the implementation of the program in question is associated with the emission of a dispersed component, which is attributed to aerosols or microdrops that form clouds. Indeed, the absorption spectrum of molecules of each type occupies a restricted range of the spectrum, in contrast to the absorption spectrum of particles or droplets in the entire spectral region. Therefore, water microdroplets fill the holes in the absorption spectrum of molecules in the atmosphere [11, 12]. In this regard, although the total mass of atmospheric aerosols-droplets is a fraction of a percent of the mass of atmospheric water, the contribution to the atmospheric emission of this component is significant.

However, in the framework of the standard atmosphere model, i.e., an atmosphere with averaged parameters, the average humidity of the atmosphere is about 80% near the Earth's surface and decreases with an increasing altitude, i.e., condensed water phase is absent in the atmosphere. Therefore, the real amount of condensed atmospheric water is determined by fluctuations and is relatively small. To find it, we use the energy balance of the atmosphere. The subject of this article is the development of an algorithm to determine atmospheric radiation fluxes and to compare the calculation results based on this algorithm with various aspects of the global atmospheric energy, including the balance of the greenhouse components of the atmosphere and the evolution of the global temperature of the Earth.

1. GLOBAL PROPERTIES OF THE EARTH'S ATMOSPHERE

1.1. Standard Atmosphere Model

In the analysis of the long-term global evolution of the atmosphere, it is necessary to eliminate short-term fluctuations of its parameters. This is taken into account in the model of the standard atmosphere, within which the parameters averaged over the season, latitude, and longitude of the given area and time of

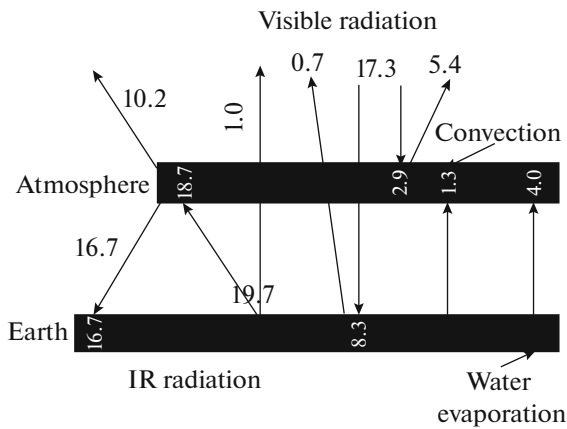


Fig. 1. Powers that the Earth receives and gives as a whole, as well as the atmosphere, as a whole, expressed in 10^{16} W; the absorbed power is indicated in the corresponding boxes, and the consumable power is marked near the arrows.

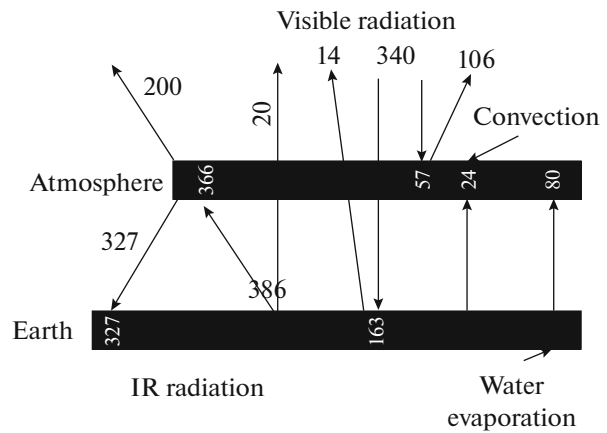


Fig. 2. Average energy flux in W/m^2 received and emitted by the Earth and the atmosphere as a whole: the absorbed flows are indicated in rectangles, and the consumable flux are near the arrows.

day are used. The atmospheric parameters will depend only on the altitude of a atmospheric layer above sea level. This averaging corresponds to the model of standard atmosphere; further, the obtained parameters of the standard atmosphere [5], which are oriented to the atmosphere of the United States, will be used. In this model, the global temperature or the average temperature on the Earth's surface is 288 K, and the temperature of the troposphere, i.e., at altitudes up to 10 km, decreases linearly with altitude, such that the temperature gradient in this region is approximately $dT/dh = -6.5$ K/km. The total molecular density at the Earth's surface is $N(0) = 2.55 \times 10^{19} \text{ cm}^{-3}$, and if the dependence of the molecular density $N(h)$ at the altitude h is approximated as

$$N(h) = N(0) \exp\left(-\frac{h}{\Lambda}\right),$$

and the scale of the change in density Λ for air molecules in the troposphere is ~ 8 km. At the same time, no distinction is made between nitrogen and oxygen molecules, the main components of air: we consider them to be identical with an average molecular weight of $m = 29$ a.u. These molecules are the buffer environment in which there are radiating molecules and water droplets.

An important role in the formation of the atmospheric greenhouse effect is played by energetic processes in the Earth's atmosphere. Figures 1 and 2 and Table 1 present the power P and energy fluxes J for processes that determine the energy balance of the Earth and its atmosphere, and $J = P/S$, where $S = 5.1 \times 10^{14} \text{ m}^2$ is the surface area of the Earth. The data in Fig. 1 for the power of the considered energetic processes are taken from [13]; they, in turn, are borrowed from the NASA report [14]. More convenient, though less accurate, characteristics are the average energy fluxes for these processes [15]. They coincide within a few percent with the parameters of the planet's energy balance contained in subsequent works, in particular, in modern books on atmospheric physics [16–24]. This coincidence suggests that, first, these works use the same source, NASA data, and second, the energy balance of the Earth as a whole has changed little over the past half century.

The character of the energetic balance of the Earth and its atmosphere is mainly subjected to the conditions of the greenhouse effect, as originally formulated by Fourier [1, 2]. Namely, the energy of solar radiation absorbed by the surface of the Earth that returns in the form of infrared radiation, and the atmosphere partially blocks this radiation. As a result, the surface temperature is higher than in the case of a transparent atmosphere for infrared radiation. Under such condi-

Table 1. Total power in the energy balance of the Earth and the Earth's atmosphere as a whole, expressed in 10^{16} W and taken from Fig. 1

	Arrival	The loss
Earth and atmosphere	$8.3 + 2.9 + 0.7 + 5.4 = 17.3$	$0.7 + 5.4 + 1.0 + 10.2 = 17.3$
Land	$8.3 + 16.7 = 25.0$	$8.3 + 16.7 = 25.0$
Atmosphere	$2.9 + 18.7 + 5.3 = 26.9$	$16.7 + 10.2 = 26.9$

tions, the infrared radiation fluxes of the atmosphere on the Earth's surface and into the surrounding space are separated, i.e., the optical thickness of the atmosphere with respect to infrared radiation is much higher than unity. For visible radiation of the Sun, which more or less freely penetrates the Earth's surface, the optical thickness is substantially less.

The basis of the energy balance of the Earth and its atmosphere is solar radiation. On average, solar radiation has a power of 3.86×10^{26} W [25], which corresponds to the temperature $T_{\text{ef}} = 5777$ K of an absolute black body. At the same time, the Sun mainly radiates in the visible and infrared regions of the spectrum; the portion of ultraviolet radiation, radio waves, and x-ray radiation accounts for less than 1% of the power. The solar flux at the level of the Earth, which is called the solar constant, is about 1365 W/m² [26–29]. Although this value is called a constant, it changes with time [30, 31] due to the nonstationary nature of solar processes, but the variations of this value are a fraction of a percent. In particular, it was 1361 W/m² in the period of the solar minimum [32]. An important role in the determination of the solar-constant variations over time is played by the accuracy of its measurement [33].

As follows from the data in Fig. 1, the solar-radiation power in the visible region of the spectrum, which is equal to 1.73×10^{17} W, penetrates the lower atmosphere of the Earth. Some of this radiation with a power of 6.1×10^{16} W is reflected from the Earth's surface, and the atmosphere and returns to the surrounding space. In addition, the atmosphere sends 1.02×10^{17} W of infrared radiation into the surrounding space, and infrared radiation with a power of 1.0×10^{16} W travels from the Earth's surface into the surrounding space. Next, the Earth's surface absorbs visible and infrared radiation with a power of 2.5×10^{17} W and emits infrared radiation 1.97×10^{17} W, and the power of infrared radiation emitted by the atmosphere and absorbed by the Earth's surface is 1.67×10^{17} W. In addition, the power of 5.3×10^{16} W is transmitted to the atmosphere from the Earth's surface, spent on maintaining the convective movement of the atmosphere, as well as the evaporation of water, which is further condensed in the atmosphere. The energy balance of the Earth and the atmosphere for the total power is also presented in Table 1.

The data presented for the energy balance of the Earth and its atmosphere can be a the basis of models that may be used to obtain estimates for the parameters of the Earth and the atmosphere as emitters. Using the model of an absolute black body for the surface of the Earth and the radiating layers of the atmosphere, we obtain the relationship between the radiation power in the infrared spectrum range P_{rad} and temperature radiators T_r according to the Stefan–Boltzmann law

$$P_{\text{rad}} = S\sigma T_{\text{rad}}^4, \quad (1)$$

where S is the area of the Earth's surface, $\sigma = 5.67 \times 10^{-8}$ W/(m² K⁴) is the Stefan–Boltzmann constant. Hence, based on the power of infrared radiation from the Earth's surface $P_{\text{em}} = 1.97 \times 10^{17}$ W, we get the average temperature of the Earth's surface $T = 287$ K. This value is slightly different from the temperature of the Earth's surface in the framework of the standard atmosphere model ($T = 288$ K) [5], and this difference also characterizes the accuracy of the models used.

Data on the energy balance of the Earth and its atmosphere can be used to determine the atmospheric parameters as a source of thermal radiation. We introduce the atmospheric optical thickness u for infrared radiation and, in our estimates, we assume that it does not depend on the radiation frequency. The probability of a signal passing through the atmosphere as it propagates perpendicularly to the Earth's surface is $P = \exp(-u)f(u)$. For convenience, the distribution function $f(u)$ over optical thickness will be assumed to be a constant in the interval $u_1 < u < u_2$, and to be zero beyond its boundaries. Based on this, we determine the probability that infrared photons pass through the atmosphere if they are isotropically created on the Earth's surface. This probability is given by the formula

$$P = \int_{u_1}^{u_2} f(u)du \int_0^1 e^{-\frac{u}{\cos\theta}} d \cos\theta, \quad (2)$$

where θ is the angle between the normal to the surface of the Earth and the direction of the photon. According to this formula for $u_2/u_1 = 1.2, 1.5, 2.3$, we find the observed probability of photon survival as it passes through the atmosphere, which, in accordance with Fig. 1, is $1/20$; it is realized with an average optical thickness of the atmosphere of [34]

$$\bar{u} = \int_{u_1}^{u_2} uf(u)du = 2.6 \pm 0.2.$$

This is the characteristic optical thickness of the atmosphere for the thermal radiation of the Earth.

Based on the thermal radiation power of the atmosphere of the Earth 1.67×10^{17} W and to surrounding space 1.02×10^{17} W, we determine by analogy with the radiation of the Earth's surface temperature of atmospheric layers T_{\downarrow} and T_{\uparrow} , which are responsible for thermal radiation in the indicated directions. Modeling the radiation of these layers as created by an absolute black body and using the Stefan–Boltzmann law (1), we obtain [34]

$$T_{\downarrow} = 276 \text{ K}, \quad T_{\uparrow} = 244 \text{ K}.$$

In accordance with the character of the change in the temperature of the standard atmosphere with an altitude, thermal radiation fluxes directed to the surface of the Earth and outside are created on average by atmospheric layers at altitudes [34]

$$h_{\downarrow} = 1.7 \text{ km}, \quad h_{\uparrow} = 6.8 \text{ km}.$$

Below we will use data obtained from the energy balance of the atmosphere to analyze its thermal radiation.

1.2. Evolution of Global Temperature

The nature of the change in the Earth's energy balance is manifested by a change in the global temperature of the Earth's surface, i.e., the temperature averaged over all geographic points of the globe. This value as a function of time is experiencing large fluctuations, and, in order to reduce the effect of daily and seasonal fluctuations, we define the global temperature of the Earth's surface as averaged over the globe and time during the year. Analysis of the global temperature is different in principle from problems of meteorology, where weather changes are determined by the movement of air, heat, and moisture. The task is to determine the indicated parameters on the basis of their values in the corresponding geographical points and at some points in time. This task can be solved on a limited time interval, which hardly exceeds 1 or 2 weeks. When analyzing the global atmospheric properties, we deal with much longer times, starting from the year. Therefore, if deterministic methods are used in the weather analysis, then the analysis of global atmospheric parameters is based on statistical methods.

The main atmospheric parameter we will focus is the global temperature and its change in time, which, in any case, exceeds years. Next, we define the global temperature of the Earth as the average temperature of the Earth's surface, for which averaging is carried out over different geographic points of the Earth, as well as over time. This value can be determined reliably if its values far exceed its fluctuations.

At the same time, measured changes in global temperature in the last 150 years are tens of fractions of a degree, while seasonal temperature changes reach several tens of degrees. Fluctuations of global temperature at each point on the Earth are measured in degrees. However, it is possible to reduce the fluctuations in question, if, when finding a change in global temperature over a certain period of time, by comparison the changes of temperatures, rather than their values that are compared at the appropriate times but changes in global temperature. This approach was developed by Hansen et al. [35]. In the framework of this approach, we take the temperature at a certain point on the Earth's surface at a given point in time and compare it with the temperature at the same point and at the same day of the year and time of day but in different years. It is clear that a change of this value from year to year is degrees, not tens of degrees, like the global temperature itself. We average this change in global temperature over all points of the globe, according to the time of day and according to the season. The resulting change in global temperature ΔT for a given time, measured in years, is the output parameter characterizing climate change. Moreover, if the global tempera-

ture fluctuation is measured in degrees, then the fluctuations of global temperature changes ΔT is estimated as 0.1 K.

Of course, the implementation of this program requires a lot of information and time-consuming work. Nevertheless, the necessary information is contained in the measurements of a large number of meteorological stations that have existed since the second half of the nineteenth century. The number of meteorological stations at the end of the 19th century was just over 6000; their number has decreased by almost three times, but basic information now follows from satellite measurements. At the same time, a comparison of changes in Earth's global temperature, which were obtained on the basis of appropriate measurements in winter and summer during daytime and night in the Northern and Southern Hemisphere with averaging of these data throughout the year shows that they do not exceed 0.2 K [36, 37] and can be considered as a fluctuation of the change of the global temperature.

Figure 3 shows the changes in the global temperature of the Earth's surface with averaging over 5 and 11 years. According to this figure, annual fluctuations to change the global temperature of the Earth ΔT make about 0.1 K. This also implies the nonmonotonic nature of the change in global temperature in the period under consideration. It was during the 1880–1910 that there was a slight cooling, which was replaced by a slight warming in 1910–1940. This was passed on to the next cooling in 1940–1950. During 1950–1980, the global temperature did not change on average, and there has been a period of warming from 1980 to the present, such that the global temperature rises monotonically. Approximating the change in global temperature of the Earth ΔT over the past 30 years by linear dependence

$$\Delta T = \frac{dT}{dt}(t - t_0), \quad (3)$$

we have from the processed data in Fig. 4 [38] $dT/dt = 0.018$ K/year, where t is the time and t_0 is the initial time. In addition, the standard deviation from the linear dependence, i.e., the global temperature fluctuation is 0.09 K according to Fig. 3

Note that the data in Fig. 3 for the global temperature are the most reliable, because they use a strict averaging of temperature over various geographic points of the Earth. Nevertheless, the temperature change in the past at a certain geographical point of the planet based on isotopic analysis of sediments [39–41] gives an idea of climate change in the past.

The temperature of this point on the planet at the moment when the considered layer has passed into deposition follows from the ratio of the concentrations of stable isotopes ^{18}O and ^{16}O , and the time of the formation of this layer can be determined both by the depth of the studied layer and by the so-called geochronological method (e.g., [42, 43]), which allowed a

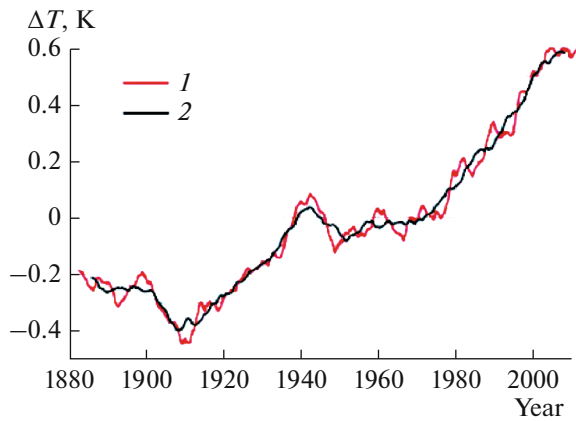


Fig. 3. Change in the global temperature of the Earth's surface from the end of the 19th to the beginning of the 21st century, obtained by averaging the corresponding values, which relate to individual geographic points and the same time points during the day and season [36, 37]; averaged over 5 (1) and 15 (2) years.

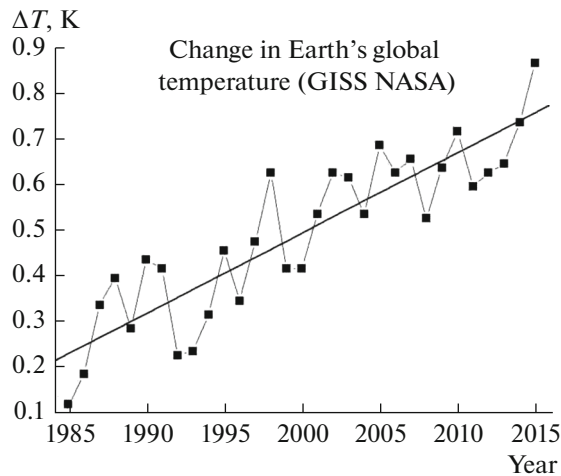


Fig. 4. Change in global temperature of the Earth's surface, obtained by averaging the corresponding values, which relate to individual geographic points and identical time points during the day and season [36, 37] over the past thirty years (points). The direct line is the averaging of these data [38].

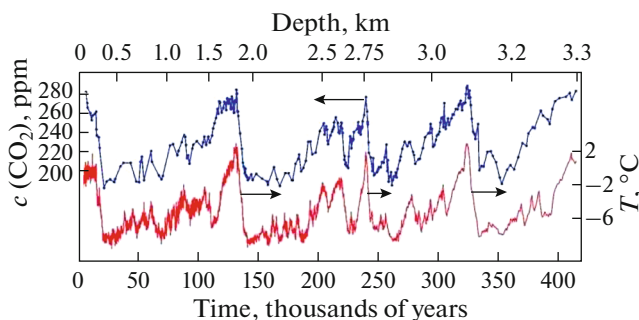
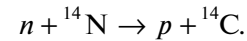


Fig. 5. Change in temperature of the Earth's surface at Vostok station (Antarctica) and the carbon dioxide concentration over the past 400000 years [47–49].

deep look into the past. This method was primarily applied to the analysis of the radioactive carbon isotope ^{14}C , the half-life of which is 5730 years, and the formation occurs under the action of cosmic neutrons according to the scheme [44–46]



This process became an important archeological tool and played a significant role in the creation and development of geochronology. For other times, when of location of the object in sediments, other isotopes are used.

As an example of local temperature measurement in the past, Fig. 5 shows its change over time in the past 400000 years at Vostok station (Antarctica). In this case, air bubbles in the ice were analyzed, the temperature was determined by the ratio of oxygen isotopes, the time was found according to the depth of the hole and calibrated by the isotope method, and the atmospheric concentration of carbon dioxide was determined by its concentration in the bubbles.

2. GREENHOUSE COMPONENTS OF THE EARTH'S ATMOSPHERE

2.1. Carbon Dioxide in the Atmosphere of the Earth

The main greenhouse components of the atmosphere are carbon dioxide and water molecules as well as microdroplets of water. Below, we consider the behavior of each of these components in the Earth's atmosphere, starting with carbon dioxide, which is in chemical equilibrium with organic compounds at the Earth. The transition between atmospheric carbon dioxide and carbon compounds on the Earth's surface is called the carbon cycle, and its channels are taken from [50–52], are shown in Fig. 6. Although the accuracy of these data is limited, the diagram below reflects the main features of the carbon cycle.

Photosynthesis is the main process for the removal of carbon dioxide from the atmosphere. This is a complex process in which plant chloroplasts are a catalyst that transfers CO_2 molecules under the influence of solar radiation in solid forms of carbon [53]. The complex nature of photosynthesis [54–59] is evidence that this process depends on the type of plant involved in it, its growth phase, and the external conditions under which this process takes place. By the nature of the photosynthesis process, plants are divided into groups C3 and C4 according to the number of carbon atoms participating in the elementary chemical process during photosynthesis [60]. For the plants of the group C3, which includes wheat, rice, and beans, the process proceeds in the course of collisions of the CO_2 molecule with an intermediate product, whereas the CO_2 molecule is first captured by the cell in the case of the C4 group, and the process then proceeds with the participation of bound molecules. This leads to different dependences of the rate of the photosynthesis process

on the conditions under which it takes place, and in particular, on the concentration of CO_2 molecules in ambient air [61]. Along with the photosynthesis process, the removal of carbon dioxide from the atmosphere over the oceans may be associated with the dissolution of carbon dioxide in the ocean, which leads to the formation of carbonate type CaCO_3 . Carbonate decomposition creates a stream of carbon dioxide in the atmosphere. Other channels for the formation of atmospheric carbon dioxide are decay processes, as well as the respiration of plants and microbes.

Human activity leads to the accumulation of carbon dioxide in the atmosphere as a result of burning fossil fuels (coal, oil, and gas), as well as carbon-containing materials. This creates most of the carbon dioxide flux in the atmosphere through human economic activity. At the same time, 35% of carbon dioxide emissions into the atmosphere are accounted for by burning coal, 36% are from oil, 20% are from methane, 3% are from carbon dioxide emissions during the manufacture of cement, and the other result from the use of wood, biofuel, etc. [62]. Along with the emission of carbon dioxide into the atmosphere in process of energy production from fuel combustion, the forest destruction in tropical regions of South America, Africa, and Asia makes a significant contribution to formation of atmospheric carbon dioxide [63–65]. Approximately $1.5 \times 10^5 \text{ km}^2$ tropical forests are destroyed annually. It is difficult to determine the effect of this process on the Earth's climate. On the one hand, the area cleaned of forest is used further in agricultural production, where photosynthesis plays a decisive role. On the other hand, forest destruction changes the nature of water evaporation from the released area. Thus, the effect of forest destruction on the Earth's climate is ambiguous.

We note the following aspect of the diagram presented in Fig. 6. At a contemporary concentration of carbon dioxide in the atmosphere, the flux of carbon dioxide in the atmosphere through all channels exceeds the total flux of carbon dioxide removed from the atmosphere, such that the concentration of CO_2 molecules in the atmosphere increases with time. However, if we exclude human activities from the carbon cycle, the concentration of CO_2 molecules in the atmosphere will decrease. It can be expected that it will drop to a limit between 260 ppm and 280 ppm, which corresponds to the values of this quantity before the industrial era. Apparently, within these limits, the considered value was retained for the previous 10000 years [66].

To the data in Fig. 6, let us add that the Earth's atmosphere presently contains approximately 8×10^{17} g carbon in the form of CO_2 molecules. For comparison, the average mass of atmospheric water is 1.3×10^{19} g, and the mass of atmospheric air is 5.1×10^{21} g. Based on the data in Fig. 6, it follows that the residence time of carbon dioxide in the atmosphere is about 4 years.

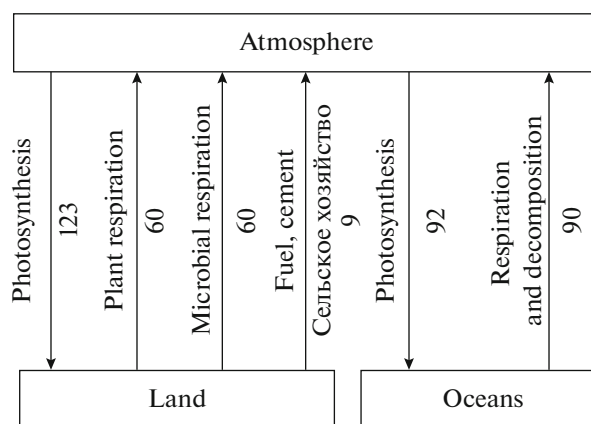


Fig. 6. Carbon fluxes through the Earth's atmosphere in the carbon cycle [50–52], expressed in 10^9 tons of carbon per year.

During this time, carbon dioxide mixes with the air in the atmosphere; thus, the concentration of CO_2 molecules in atmospheric air does not depend on a measurement point, far from carbon dioxide sources or the areas of its destruction.

Thus, the balance between atmospheric carbon dioxide and solid carbon, which is part of the organic compounds on the Earth's surface, is associated with photosynthesis and oxidation of carbon-containing substances, mainly as a result of the rotting and respiration of plants. As can be seen from the above data, the contribution of human industrial activity to the formation of atmospheric carbon dioxide is approximately 5%. Thus, carbon dioxide emissions in the atmosphere as a result of carbon energy are not as significant as the media assure us.

The most complete information on the current concentration of CO_2 molecules in the atmosphere and its evolution follows from the measurements of the Mauna Loa Observatory, Hawaii, United States [67–70]. This observatory is conveniently located at an altitude of 3400 m above sea level, which excludes the influence of sources of atmospheric CO_2 and makes it possible to operate with a stable concentration of carbon dioxide in atmospheric air. In addition, the monitoring of the atmospheric carbon dioxide concentration occurs continuously, starting from 1959. Its results are presented in Fig. 7 with monthly or annual averaging of the concentration of carbon dioxide molecules [69, 70].

According to Fig. 7, the concentration of CO_2 molecules in the atmosphere changed from 316 ppm in 1959 to 410 ppm in 2017 ($1 \text{ ppm} = 10^{-6}$), i.e., over the past 60 years, it has increased by 30%. Figure 7a shows that the concentration of CO_2 molecules in the atmosphere grows with acceleration. Indeed, the rate of accumulation of CO_2 molecules in the atmosphere changed from 0.7 ppm per year in 1959 to about 2.1 ppm per year

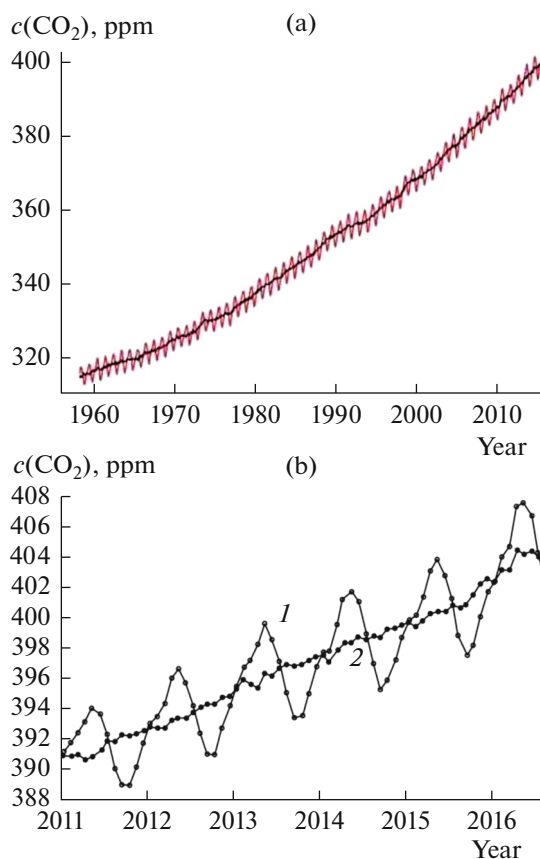


Fig. 7. Concentration of carbon dioxide in atmospheric air as measured by the Mauna Loa Observatory [68, 69] during the last half-century (a) and recent years (b) (1) average values for the corresponding month, (2) averaging over measurements for 6 months before and after this time.

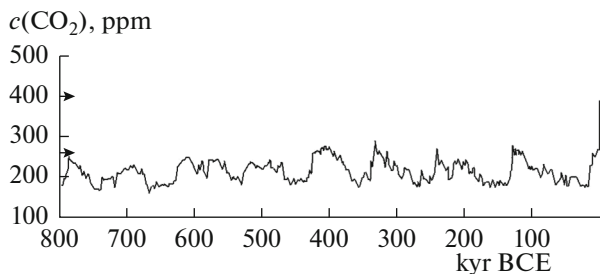


Fig. 8. Concentration of carbon dioxide in the Earth's atmosphere in the past, recovered from the analysis of glacier ice [70].

in 2017. Seasonal variations in the concentration of CO_2 molecules in the atmosphere (Fig. 7b) occur due to the higher intensity of photosynthesis in the Northern Hemisphere as compared to that of the Southern Hemisphere. As a result, the measured concentration of carbon dioxide molecules decreases in the period from May to September, when photosynthesis takes place in the Northern Hemisphere.

The average annual increase in the atmospheric concentration of carbon dioxide is currently 2.1 ppm

per year, which corresponds to the burning of 4.4×10^9 tons of carbon. This is half of the amount of carbon contained in fossil fuels extracted during the year (coal, oil, and methane). From Fig. 7b it follows that the atmospheric concentration of carbon dioxide decreased from 402 ppm to 395 ppm from May to September 2014 and then increased to 404 ppm from September 2014 to May 2015. This corresponds to a transition of 15×10^9 tons of carbon from the atmosphere in the first case and a transition of 19×10^9 tons of carbon to the atmosphere in the second case. Thus, there is information on the modern content of carbon dioxide in the atmosphere and the rate of its change.

Along with monitoring of the current carbon dioxide content in the atmosphere, a certain understanding of the evolution of this parameter in the past follows from analysis of the carbon dioxide content in glacial deposits. Figure 8 shows the change in the carbon dioxide concentration in the past [71]. Leaving aside the periodic character of oscillations of this magnitude, we note that the average carbon dioxide concentration is close to its value in our era in the preindustrial era.

Thus, at present, the atmospheric carbon dioxide concentration c grows at a rate of about 2.4 ppm per year, which corresponds to equation [38]

$$\frac{d \ln c}{dt} = 0.006 \text{ year}^{-1}, \quad (4)$$

where the current concentration of atmospheric carbon dioxide is assumed to be $c = 410$ ppm. It follows that, with a modern growth rate of the atmospheric concentration of CO_2 molecules, this value will double in about 120 years. Further, in accordance with the Arrhenius concept [6], which is based on the use of the atmospheric concentration of CO_2 molecules as characteristics of the current state of the atmosphere, we find that, according to formula (3), doubling of the concentration of carbon dioxide in the atmosphere leads to a change

$$\Delta T = (2.0 \pm 0.3) \text{ K}. \quad (5)$$

Note that this result follows from measurements in the framework of NASA programs, and the increase in the carbon dioxide concentration is not in this case the cause of the change in global temperature but is used as a characteristic of the atmospheric state.

Let us check the Pauling concept, which relates to the change in atmospheric concentration of carbon dioxide to the change in global temperature [72, 73]. Moreover, a specific channel of this connection was indicated. It is carbon dioxide that is mainly absorbed by the oceans; it exists in the oceans as a compound of the type CaCO_3 as a result of chemical equilibrium



and the enthalpy for this process or the binding energy of CO_2 molecules is $\Delta H = 178 \text{ kJ/mol}$ [74]. Since the number of bound carbon dioxide molecules in the

ocean is about 60 times more than its amount in the atmosphere, the ocean in this equilibrium can be considered a source of carbon dioxide; thus, the dependence of the concentration of atmospheric carbon dioxide c on the ocean temperature T has the form $c \sim \exp(-\Delta H/T)$, which, on the basis of formula (3), gives

$$\frac{d \ln c}{dt} = \frac{\Delta H}{T^2} \frac{d\Delta T}{dt} = 0.0046 \text{ year}^{-1}.$$

Comparison with formula (4) shows the validity of the concept of Pauling, i.e., the chemical equilibrium between oceanic and atmospheric carbon dioxide is largely responsible for the observed increase in carbon dioxide concentration.

2.2. Atmospheric Water

Another atmospheric greenhouse component, water, enters the atmosphere as a result of evaporation of water molecules from the Earth's surface and precipitation. The total rate of water evaporation from the Earth's surface is 3.9×10^{20} g/year [75–78], and the same amount of water returns to Earth annually as precipitation, with only about 1.0×10^{18} g/year in the form of snow. Figure 9 presents the balance of water in the processes of its transitions between the land, oceans, and the Earth's atmosphere. The average water content in the atmosphere is 1.3×10^{19} g [79–84] as compared to a mass of 5.1×10^{21} g for atmospheric dry air. This corresponds to an average concentration of water molecules in atmospheric air of 0.33%, and to an average concentration of 1.7% near the Earth's surface. It also follows from these data that the average residence time of water molecules in the atmosphere is approximately 9 days [78]. To this we add that water, distributed in the atmosphere, is nonuniform, and its content in a given area of the atmosphere changes with time.

At the same time, atmospheric water makes up a small fraction of the Earth's water, 96% of which is salty; the fresh water content is about 1.0×10^{22} . If the atmospheric water is transferred to a liquid state and is distributed over the Earth's surface uniformly the height of the layer of liquid water will be 2.5 cm [83]. Further, the average water density in the atmosphere near the Earth's surface is 3 g/m^3 as compared to a dry air density of 1.2 kg/m^3 . This corresponds to an average partial pressure of water vapor at the Earth's surface, which is equal to about 2 Torr. Since the pressure of a saturated water vapor at a temperature of 0° is 4.7 Torr [84, 85]. The surface areas of the atmosphere located at altitudes at least below 3 km contain water in the form of free molecules under equilibrium conditions.

Other phase forms of water—liquid, snow, and ice (crystalline)—form and mainly exist in the higher atmospheric layers. Atmospheric particles, including the water in these phases, are called aerosol particles or aerosols. Processes involving aerosols [86–91] affect

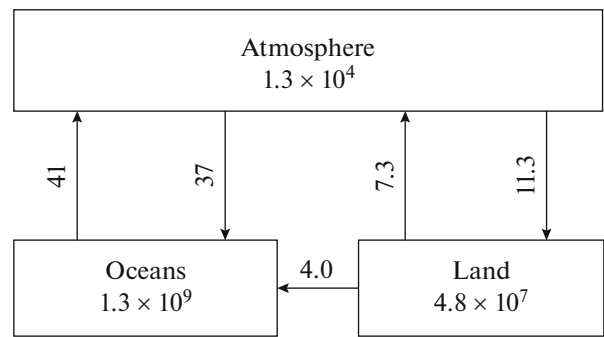


Fig. 9. Rate of exchange of water between land, ocean, and atmosphere, expressed in 10^{18} g/year, presented near the corresponding arrows; the water content in each of the objects is given in 10^{15} g (billion tons).

various atmospheric properties, including electrical and optical properties, and the participation of aerosols in atmospheric electrical phenomena is of key importance [92].

Since the tropospheric temperature decreases with an increasing altitude in the layers of the troposphere where the pressure of atmospheric water vapor exceeds the pressure of saturated steam at a current air temperature, it is possible for the condensation of excess vapor of atmospheric water to form growing aerosols, i.e., micron-sized, liquid water particles. In particular, the typical parameters of water microdroplets in a ripe cumulus cloud are [93–96]

$$r_0 = 8 \mu\text{m}, \quad N_d = 10^3 \text{ cm}^{-3},$$

where r_0 is the average aerosol radius and N_d is the average microdroplet number density. In accordance with this formula, the average micro droplet contains about 7×10^{13} water molecules, and the average number density of bound molecules of microdrops of a cumulus cloud is $7 \times 10^{16} \text{ cm}^{-3}$, whereas the average density of free water molecules at the Earth's surface is $4.3 \times 10^{17} \text{ cm}^{-3}$.

The Earth's atmosphere contains various types of aerosol particles in a wide range of sizes from 0.01–100 μm that can affect various atmospheric properties. These aerosols are usually based on water, but they may also contain SO_2 , NH_3 , NO_x , mineral salts, and other compounds resulting from processes on the Earth's surface. The aerosol content in the atmosphere is of interest for the analysis of atmospheric radiative properties in the infrared range of the spectrum; however, the aerosol concentration in the air is unstable. The presence of water in the atmosphere in the condensed phase, i.e., in the form of aerosols, could possibly provide a measurement of the water content in the stratosphere. Indeed, it was previously shown that water barely penetrates the upper layers of the troposphere, because condensation occurs due to the low temperature of water. Reaching micron sizes, aerosols fall under the action of gravitational force.

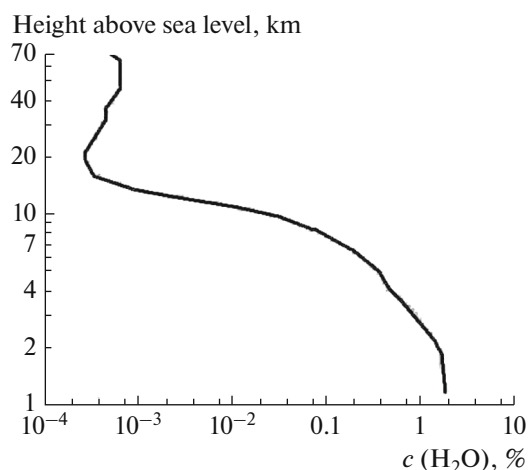


Fig. 10. Dependence of the concentration of water molecules in atmospheric air on altitude [97].

However, a small portion of the water remains in the form of free molecules. For example, at -20°C , the density of free molecules at a pressure of saturated water vapor is $3 \times 10^{16} \text{ cm}^{-3}$ [84]. Therefore, water vapor penetrates to the stratosphere to a small extent, where it does not condense due to the temperature, which is higher than that in the tropopause. Since it mixes with air molecules as a result of convective air movement, the concentration of water vapor in the stratosphere may indicate both the aerosol content in the upper troposphere and the temperature distribution in the atmosphere over the altitude.

As can be seen, the aerosol formation in the atmosphere leads to a sharp drop in the density of water molecules in the troposphere with increasing altitude. In particular, Fig. 10 shows the dependence of the concentration of water molecules with respect to air molecules for one of the measurements in a tropical atmosphere under conditions in which the concentration of water molecules in the near-surface atmosphere substantially exceeds its average value. The atmospheric water content drops sharply with altitude, and the concentration of water molecules in the stratosphere is much less than that of carbon dioxide, in contrast to the ratio between them in the troposphere. Long-time measurement of the content of stratospheric water can give a parameter characterizing the presence in the atmosphere of the main source of its thermal radiation. For example, long-term balloon measurements of the stratospheric water content were carried out in Boulder, Colorado. Let us present their results from 1980 to 2010 at altitudes of 16–26 km [98]. During this period, the stratospheric water content increased on average by $1.0 \pm 0.2 \text{ ppm}$ or $(27 \pm 6)\%$. Moreover, during 1980–1989, this increase ranged from $0.44 \pm 0.13 \text{ ppm}$ at altitudes of 16–18 km to $0.07 \pm 0.07 \text{ ppm}$ at altitudes of 24–26 km. In the period 1990–2000, the increase in the content of stratospheric water averaged at other altitudes was $0.57 \pm$

0.25 ppm , it decreased on average by $0.35 \pm 0.04 \text{ ppm}$ whereas in the period 2001–2005, increasing again in 2006–2010 on average, by $0.49 \pm 0.17 \text{ ppm}$. We note here that the concentration of water molecules that in the stratosphere is almost three orders of magnitude lower than that in the near-surface layers of the atmosphere. It can be seen that even the concentration of stratospheric water averaged over a large period of time behaves irregularly, which indicates the complexity of the processes involving water molecules in the atmosphere. The water content in the troposphere, where water is the main source of thermal radiation also varies irregularly, since the condensation processes are added to processes involving water molecules in the stratosphere and lead to formation water microdrops which form clouds.

3. ATMOSPHERIC AIR ABSORPTION COEFFICIENT

3.1. A Simple Model of the Radiation of the Earth's Atmosphere

The radiative properties of the Earth's atmosphere are mainly associated with the presence of three components in it: molecular water and carbon dioxide, as well as water microdroplets, i.e., micron-sized water particles that form clouds. The thermal radiation of the atmosphere, which is created by the molecules in it, is due to radiative transitions between vibrational and rotational states of molecules. Leaving aside the selection rules for these transitions [99–105], which constitutes a specific section of molecular spectroscopy, we focus on the determination of absorption coefficients of atmospheric air with an admixture of optically active molecules.

In this case, the subsequent transitions are combined into bands, which makes this molecule optically active in a certain range of the spectrum. If we model the radiating regions of the atmosphere with an absolute black body, then, according to the Wien law [106, 107], the maximum of the radiation intensity corresponds to the wavelength λ_m , which is connected with the radiative temperature T by the relation $\lambda_m T = 0.29 \text{ cm K}$. Since thermal radiation is generated by atmospheric regions with a temperature of 220–300 K, wavelengths of $\lambda = 10\text{--}15 \mu\text{m}$ are of primary interest for thermal radiation of the atmosphere. Note that this corresponds to a radiative transition for a CO_2 molecule between the ground and lower vibration-excited states.

There are various forms of photon propagation in a gaseous medium, including planetary atmospheres, depending on the conditions under which this occurs (e.g., [107–111]). In this case, we are dealing with a radiating gas that is in thermodynamic equilibrium due to high air pressure. This means that photon-emitting excited molecules are not formed as a result of photon absorption but from their collisions with surrounding molecules. In other words, the tempera-

ture of the radiation generated in a certain region of the atmosphere coincides with the temperature of this layer. In addition, the optical thickness of the gas system is large, i.e., the photon-path length is small compared with the size of the system.

In the case of radiation of an optically thick layer of a gas of the same temperature, the radiative flux corresponds to the radiation of an absolute black body with a radiative temperature equal to the layer temperature. One can reduce atmospheric radiation, the temperature of which decreases with an altitude, can lead to the emission of a uniform atmosphere, and T_ω for a given frequency ω coincides with the layer temperature at which the optical thickness u_ω to the atmosphere boundary is [112, 113]

$$u_\omega(T_\omega) = \frac{2}{3}. \tag{7}$$

This result corresponds to decomposition of the partial radiation flux for a given frequency in a small parameter, which is proportional to the square of the temperature gradient. For the standard atmosphere of the Earth, this parameter is 0.01.

Let us consider the nature of the atmospheric radiation based on a simple model that takes into account that the density of molecular optically active components of atmospheric air may decrease with increasing altitude. We use a simple approximation for the photon-absorption coefficient k_ω at a given frequency ω by atmospheric air [34]

$$k_\omega = \frac{du_\omega}{dh} = A \exp\left(-\frac{h}{\Lambda}\right)$$

and define the parameters A and Λ from the condition that the optical thickness for the effective layer responsible for radiation in this direction is $2/3$. The conditions in this case, with formula (7) taken into account, are

$$\int_0^{h_1} du = \frac{2}{3}, \quad \int_{h_1}^{\infty} du = \frac{2}{3}.$$

The solution of these equations gives [34]

$$A = 0.46 \text{ km}^{-1}, \quad \Lambda = 5.3 \text{ km}, \quad u = 2.4.$$

The considered model is suitable for a molecular gas due to the monotonous decrease of the absorption coefficient with altitude and for an optically dense atmosphere $u \gg 1$; thus, the atmospheric regions responsible for the atmospheric emission towards the Earth's surface and outside it are separated. Below, we focus only on the atmospheric radiation directed to the Earth's surface.

3.2. Emission of Atmospheric CO₂ Molecules and H₂O

At the first stage of analysis of the emission of atmospheric air with an admixture of optically active components, we determine the absorption coefficient of the atmosphere at a given frequency. In this case, we are based on the data from the HITRAN databank [8–

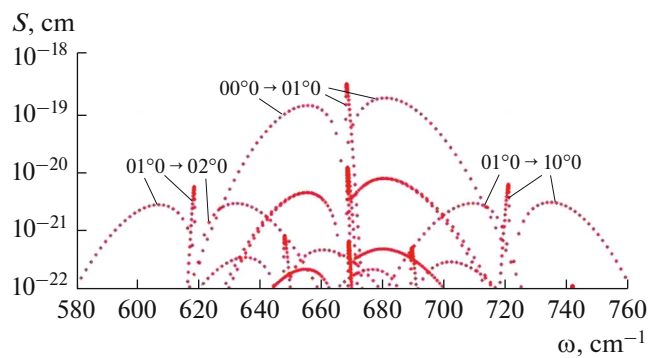


Fig. 11. Intensity of absorption rates of carbon dioxide molecules at room temperature [9, 10]; the vibrational transitions are shown to which this rotational branch belongs.

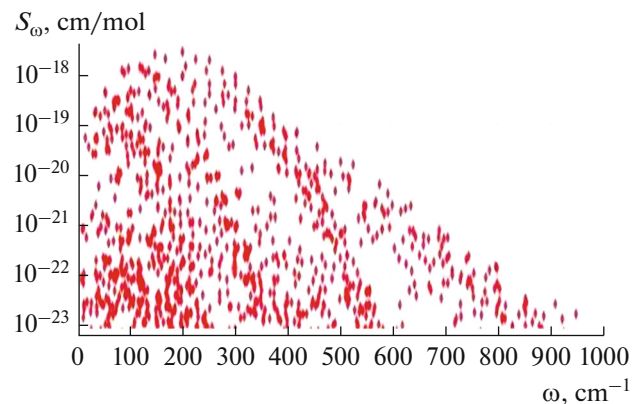


Fig. 12. Intensity of absorption of water molecules at room temperature [9].

10], which contains the parameters of a large number of vibration–rotation transitions of molecules. One of the parameters of interest is the intensity of the spectral line S_i , which is introduced such that the absorption coefficient k_ω of this component at a given frequency ω is determined by the relation

$$k_\omega = N_m \sum_i S_i a(\omega - \omega_i), \tag{8}$$

where N_m is the total density of molecules of this type, frequency ω_i refers to the center i th spectral line, and $a(\omega - \omega_i)$ is the frequency distribution function of photons, which is determined in the case of atmospheric air by collisions of the emitted molecule with air molecules and has the form

$$a(\omega - \omega_i) = \frac{\nu_i}{2\pi \left[(\omega - \omega_i)^2 + (\nu_i/2)^2 \right]}, \tag{9}$$

where ν_i is the width of the corresponding spectral line. The parameters of this formula are taken from the HITRAN databank [8–10] to calculate the absorption coefficients of the optically active components of the atmosphere. Figures 11 and 12 contain the intensity of the spectral lines for water molecules and carbon dioxide.

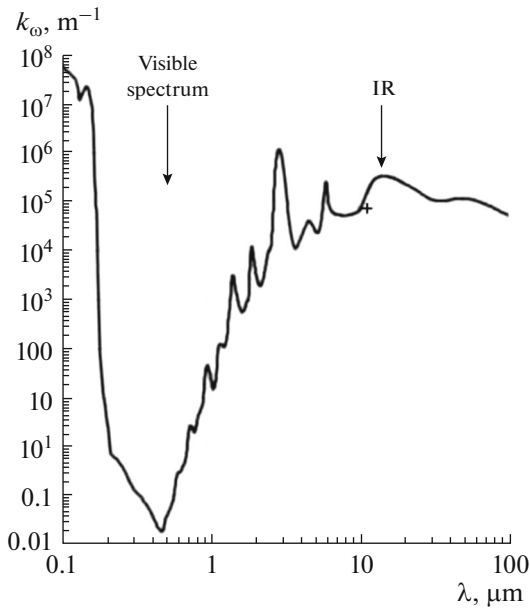


Fig. 13. Absorption coefficient of the water layer under normal conditions [114]. The cross corresponds to the atmospheric experiment [115].

The model used for the frequency-independent absorption coefficient does not describe the emission of water vapor and carbon dioxide, since the emission of molecules is concentrated in a restricted range of the spectrum, but it is suitable for water microdroplets with an appropriate distribution in a space. Indeed, the absorption cross section of photons by a black spherical particle, the radius r_0 significantly exceeds the radiation wavelength λ , the absorption cross-section is $\sigma = \pi r_0^2$, which corresponds to the absorption coefficient k_ω , independent of the wavelength of the radiation and is defined by the formula

$$k_\omega = N_d \pi r_0^2, \quad r_0 \gg \lambda, \quad (10)$$

where N_d is the particle number (microdroplets) density. The typical parameters of water microdroplets in a thundercloud are given by formula (6). It can be seen that clouds can be effective atmospheric radiators.

Figure 13 contains the dependence of the absorption coefficient of liquid water on the radiation wavelength. This figure also shows the result of the absorption study for the real atmosphere [115], according to which the absorption coefficient for radiation with a wavelength of 10–12 μm by stratocumulus clouds is 700–1000 cm^2/g . Although the applicability criterion of formula (10) is not fulfilled, it describes an experiment with a restricted accuracy. Based on the data in Fig. 13, we note the following behavior of water microdroplets in the atmosphere. The absorption coefficient of infrared radiation by a layer of liquid water is approximately seven orders of magnitude higher than its typical value in the visible spectral range. There-

fore, when microdroplets are formed from water molecules and do not contain impurities, they are transparent for visible light, but they are effective emitters in the infrared range of the spectrum. Subsequently they become visible due to the absorption of impurities or salts that stick to them.

A peculiarities of the absorption of atmospheric molecules is that the distance between neighboring spectral lines $\Delta\omega_i$ considerably exceeds the width of an individual spectral line ν_i , which is proportional to the number density of air molecules. For example, in the case of CO_2 molecules, the frequency difference for neighboring transitions is 1.56 cm^{-1} , whereas the spectral line width at atmospheric pressure is close to 0.15 cm^{-1} . Accordingly, the absorption coefficient as a function of frequency has an oscillating structure with maxima at the centers of spectral lines and minima between them.

In the case of carbon dioxide molecules, the regular model is valid [116], where the frequency differences for neighboring transitions are identical. Then, since, in the main frequency range of the transition, the rotational moment of the initial and final states is large and the intensity weakly depends on the rotational number, the intensity of the transitions S_i can be replaced by the slowly varying frequency function S_ω and, on the basis of the Mittag–Leffler theorem [117], the summation over rotation numbers in formula (8) can be performed for each frequency. The resulting expression for the absorption coefficient of a molecular gas (e.g., [118–121]) in terms of formula (8) is

$$k_\omega = \frac{N_m S_\omega}{\Delta\omega} \varphi(\omega), \quad (11)$$

$$\varphi(\omega) = \frac{\sinh(z)}{\cosh(z) - \cos\left(\frac{2\pi(\omega - \omega_0)}{\Delta\omega}\right)}, \quad z = \frac{\pi\nu}{\Delta\omega},$$

where $\Delta\omega$ is the frequency difference for neighboring transitions, ν is the width of the spectral line, and frequency ω_0 corresponds to the frequency of the vibration transition.

Figure 14 shows the frequency dependence for the absorption coefficient of CO_2 molecules in the atmosphere near the Earth's surface in the spectral range near the absorption band boundary, and Fig. 15 shows this dependence for the total absorption band. The interaction and competition of different greenhouse components occurs in the spectral range, where each of these components contributes to the total absorption coefficient. For molecules of carbon dioxide and water, competition takes place in the range of the absorption of molecules of carbon dioxide; this follows from Fig. 16, which contains the total absorption coefficient. In the frequency range with strong absorption by water molecules, their spectrum is reduced to a regular model.

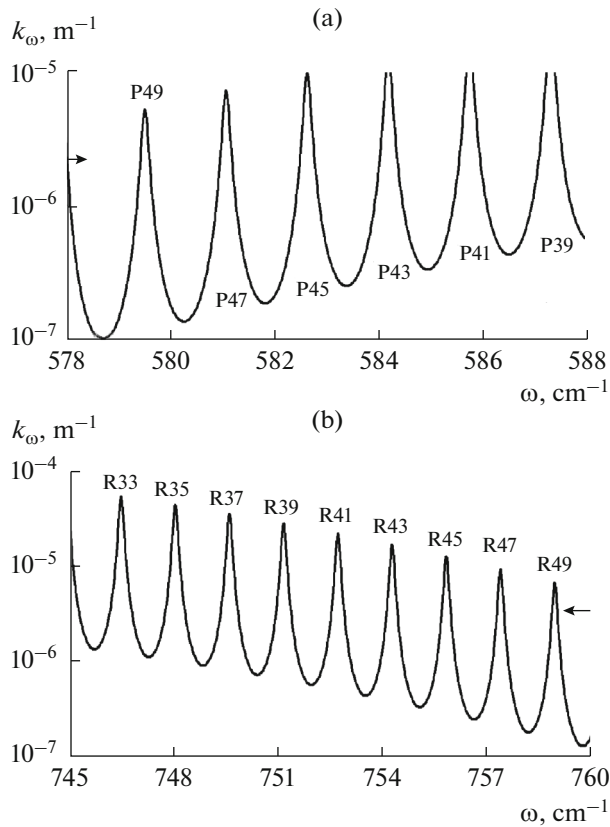


Fig. 14. Atmospheric absorption coefficient near the Earth's surface due to carbon dioxide molecules near the red (a) and violet (b) boundaries of the absorption band: the rotational moments for the initial state of the excitation process are indicated; P and R denote the corresponding rotational branch of the rotation–vibration transition.

4. ATMOSPHERIC RADIATION FLUXES TOWARDS THE EARTH

4.1. Peculiarities of Radiation of Atmospheric Air

Our goal is to create an algorithm for calculation the radiative flux of energy directed from the Earth's atmosphere to its surface. This flux is one of the components of the Earth's energy balance and determines the greenhouse effect of the atmosphere. Let us consider this effect for a standard atmosphere, i.e., for the atmosphere with averaged parameters. We note the connection between the processes of radiation and absorption, the rates of which are related by the Kirckhoff laws. Therefore, in the analysis of radiation processes, it is possible to use equally parameters describing both radiation and absorption. Apparently, the most suitable for this purpose are the coefficient of absorption of atmospheric air κ_ω and optical layer thickness u_ω for photons of this frequency. In particular, the radiation temperature at this frequency is equal to the layer temperature, the optical thickness of which is on the order of magnitude in accordance with (7).

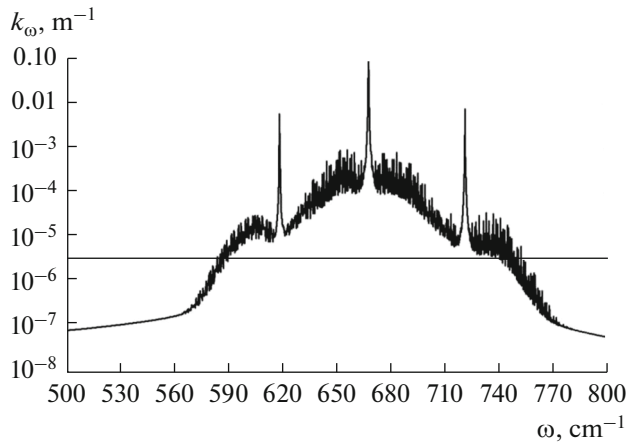


Fig. 15. Absorption coefficient of atmospheric carbon dioxide molecules near the surface of the Earth [115].

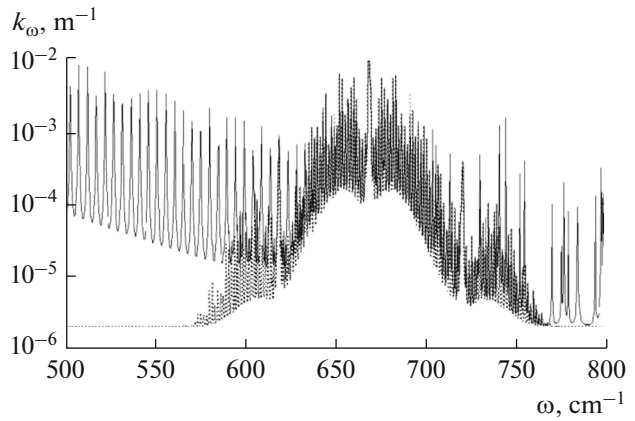


Fig. 16. Total absorption coefficient of atmospheric carbon dioxide molecules, water molecules, and water microdroplets (solid curve) near the Earth's surface in the carbon-dioxide absorption band; the points are the absorption coefficient of carbon dioxide molecules and water microdroplets.

Moreover, since atmospheric air contains three main radiating components, i.e., carbon dioxide, water molecules, and water droplets, the absorption coefficient of atmospheric air K_ω is the sum of the absorption coefficients of these components [122]

$$K_\omega = k_\omega + \kappa_\omega + \chi, \tag{12}$$

where k_ω is the coefficient of absorption by molecules of carbon dioxide, κ_ω is the absorption coefficient of water molecules, and χ is the absorption coefficient of water droplets. If we assume that the density of elementary radiators does not depend on the altitude, then, in accordance with (7), the altitude of the layer responsible for the radiation of the atmosphere at a given frequency is

$$h_\omega = \frac{2}{3K_\omega}.$$

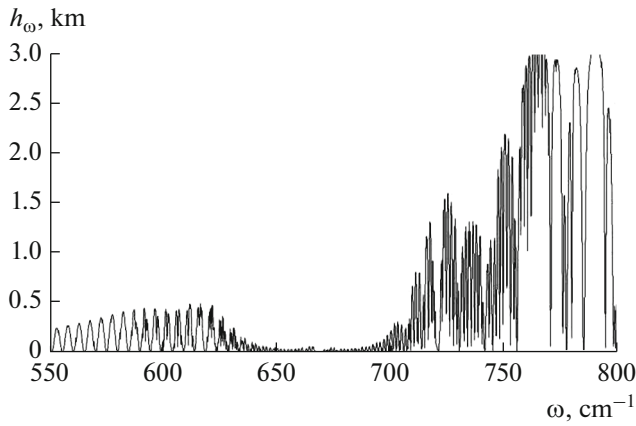


Fig. 17. Altitude of the atmospheric layer above the Earth’s surface, which is responsible for the atmospheric emission in the absorption band of carbon dioxide.

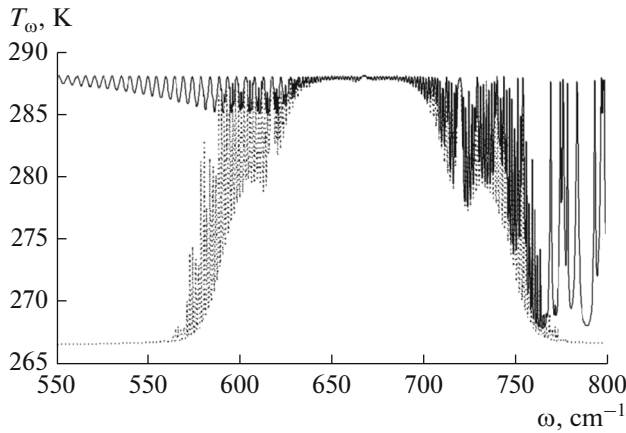


Fig. 18. Radiative temperature of the atmosphere in the absorption band of carbon dioxide (solid curve); the points are the absorption coefficient of carbon dioxide molecules averaged over the spectrum.

These conditions are valid at frequencies less than about 750 cm^{-1} in the absorption band of water molecules and carbon dioxide. Figure 17 shows the altitudes responsible for atmospheric emission in the absorption band of carbon dioxide.

Under the considered conditions, and according to the temperature gradient of the standard atmosphere in the troposphere is -6.5 K/km , we have for the radiative temperature

$$T_\omega = T_E - \frac{T_o}{K_\omega}, \quad T_o = 4.33 \frac{\text{K}}{\text{km}}, \quad (13)$$

where $T_E = 288 \text{ K}$ is the temperature of the Earth’s surface for the standard atmosphere and K_ω is the total absorption coefficient of the atmosphere. Figure 18 shows the absorption coefficient of the standard atmosphere in the range of the carbon dioxide absorption band.

The radiation temperature T_ω for a given frequency of photons makes it possible to determine the partial radiation flux

$$J_\omega = \frac{\hbar\omega^3}{4\pi^2 c^2} \left[\exp\left(-\frac{\hbar\omega}{T_\omega}\right) - 1 \right]^{-1}. \quad (14)$$

The expressions for the atmospheric radiation parameters correspond to the frequencies for which the optical thickness of the air is large and at which the radiation is generated by water and carbon dioxide molecules. It follows from Figs. 12 and 16 that, at low frequencies, the absorption of the standard atmosphere is determined by water molecules, and the absorption band of carbon dioxide molecules, according to Fig. 15, lies in the frequency range of about $580\text{--}750 \text{ cm}^{-1}$. In this case, at the lower boundary of this absorption band, the overlapping of the spectra of water and carbon dioxide takes place. Further, we will assume that molecular emission dominates at photon frequencies below 760 cm^{-1} , whereas the atmospheric radiation is determined by water droplets at higher frequencies.

4.2. Atmospheric Radiation towards the Earth

The analysis makes it possible to formulate a more accurate and realistic model of infrared radiation from the atmosphere towards the Earth while maintaining the principles inherent in previous models. Namely, we divide the frequency range of radiation into two parts, the boundary of which is approximately $\omega_o = 760 \text{ cm}^{-1}$. In the lower frequency range, the atmospheric emission is determined by the emission of water and carbon dioxide molecules, and the radiation flux is determined by the considered scheme. Within the framework of this scheme, it is given by formula (14), and the corresponding radiative temperature is calculated by formula (13). At high frequencies, the atmospheric radiation is determined by clouds containing microdroplets with temperature T_d . As a result, we have for the radiation flux of a standard atmosphere

$$J_\downarrow = \int_0^{\omega_o} d\omega \frac{\hbar\omega^3}{4\pi^2 c^2} \left[\exp\left(-\frac{\hbar\omega}{T_\omega}\right) - 1 \right]^{-1} + \int_{\omega_o}^\infty d\omega \frac{\hbar\omega^3}{4\pi^2 c^2} \left[\exp\left(-\frac{\hbar\omega}{T_d}\right) - 1 \right]^{-1} + \delta J, \quad (15)$$

where δJ is the radiation flux due to water molecules in the high frequency range. Figure 19 shows the radiative fluxes between the atmosphere and the Earth. These fluxes are elements of the Earth’s energy balance.

It follows from Fig. 19 that water molecules are partially absorbed in the high frequency region. Figure 20 shows the optical thickness of the standard atmosphere due to water molecules in this region of the spectrum. It is obtained on the basis of spectroscopic data from the HITRAN databank. In this case, we can assume that water molecules are below the clouds, i.e.,

the radiation of the atmospheric microdroplets does not shield the molecular radiation. Representing the radiation of water molecules in a given spectral range in the form of single lines, we obtain the contribution to the radiative flux due to water molecules $\delta J = 5 \text{ W/m}^2$, as shown in Fig. 19.

Formula (15) demonstrates the significant contribution of water microdroplets to atmospheric radiation. This follows from general considerations, since the absorption band of the most efficient optically active molecules is limited [11, 12], while macroscopic particles are emitted in a wide spectral range. Therefore, aerosol particles in the atmosphere are emitted in a wide spectral range [119–121], filling the transparency windows for atmospheric molecules. From the point of view of the radiative properties of the atmosphere, the radiation processes of aerosols are overlapped on the atmospheric processes of condensation and chemical processes, as well as chemical atmospheric processes and transport processes that are associated with convective transport of atmospheric air [123–131].

Among aerosols, water drops play the largest role for a number of reasons. Firstly, water is a widely spread component of the atmosphere that is capable to generate infrared radiation. Secondly, it is in the troposphere at low altitudes that effective condensation of water occurs, leading to the formation of micron-sized particles, and it is this size that is most effective for radiation, since it corresponds to the typical wavelength of thermal radiation. Since water droplets form clouds, the problem of aerosol radiation can be related to cloud behavior.

Note that the radiative flux of the atmosphere towards the Earth due to water microdroplets can be determined on the basis of the energy balance of the Earth; thus, the flux of infrared radiation from the atmosphere to the Earth's surface is

$$J_{\downarrow} = 327 \frac{W}{m^2}.$$

This gives the value given in Fig. 19 for the radiation flux to the Earth's surface created by cloud droplets. This determines the cloud temperature, which is approximately equal to $T_d = 265 \text{ K}$; this corresponds to an altitude of radiators as of $h = 3.5 \text{ km}$.

Based on the energy balance of the standard atmosphere shown in Fig. 2, we determine the optical cloud thickness. According to the energy balance of the Earth, the radiative flux of the Earth $J_s = 20 \text{ W/m}^2$ is not absorbed by the atmosphere. Obviously, this occurs in the high-frequency range, where the absorption is determined by water microdroplets. In this range of the spectrum, the Earth's surface emits flux of radiation $J'_E = 163 \text{ W/m}^2$; thus, the probability of the survival of a photon emitted by the Earth's surface in this spectrum range is equal to $P = J_s/J'_E = 0.13$. Conversely, the probability of photon survival during passage through

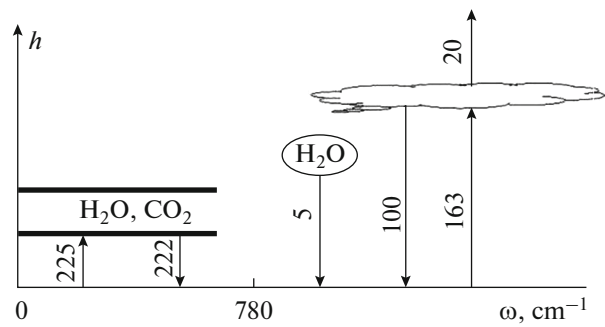


Fig. 19. Radiative fluxes from the atmosphere to the Earth and from the Earth's surface to the atmosphere, expressed in W/m^2 .

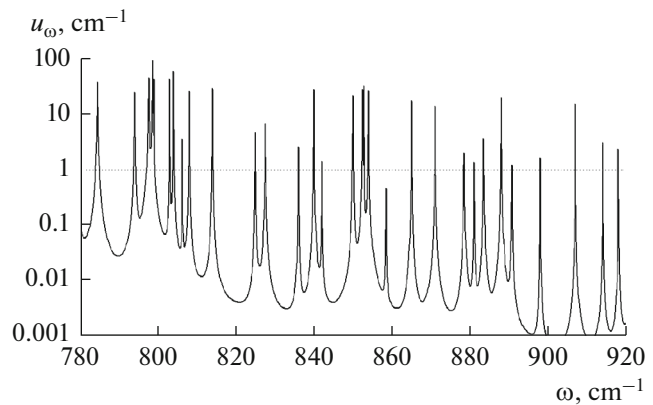


Fig. 20. Optical thickness of the standard atmosphere created by water molecules.

the atmosphere is given by formula (2). Thus, using the simplest distribution function over optical thicknesses $f(u) = \exp(-u/u_0)$, we have the following expression for the photon-survival probability:

$$P = \int_0^1 \frac{\cos \theta d \cos \theta}{u_0 + \cos \theta}.$$

The solution of $P = 0.13$ gives $u_0 = 3.2$. This value refers to the standard atmosphere, while large fluctuations correspond to the clouds and their constituent water microdroplets. Therefore, in reality, the atmospheric optical thickness in the range of the absorption band of carbon dioxide may vary significantly at different geographical points of the planet and at different times.

4.3. Cosmic Rays in the Atmosphere

The above scheme for determination of the radiative flux towards the Earth allows one to understand the peculiarities of the formation of this flux and to find the average contribution to each of the greenhouse components, which include carbon dioxide and water molecules, as well as water microdroplets. It can

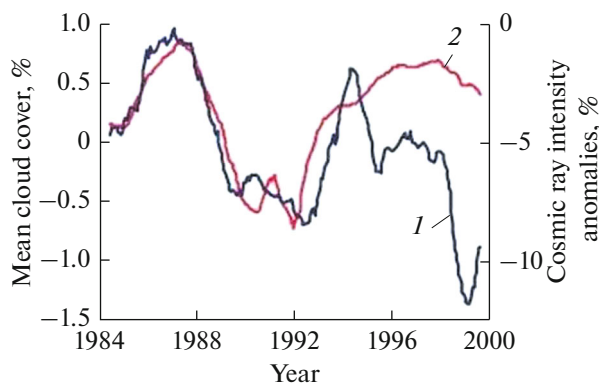


Fig. 21. Correlation between the anomalies of the cosmic-ray flux and the change in cloudiness in the lower atmosphere [134]: (1) deviations from the average for the cosmic-ray flux, (2) the same for the average atmospheric cloudiness.

be seen from Fig. 19 that the main contribution to the thermal radiation of the atmosphere comes from atmospheric water and microdroplets, which account for tenths of a percent of atmospheric water and provide one third of the radiation flux. This indicates the importance of condensation processes in the formation of the radiative flux from the atmosphere, i.e., changes in the rates of these processes can change the energy balance of the Earth.

This fact is akin to the influence of cosmic-ray intensity on the heat balance of the Earth via cloud formation. As early as 1959, it was noted [132] that an increase in the intensity of cosmic rays leads to an increase in the ionization rate in the atmosphere. This, in turn, accelerates the process of water-vapor condensation with microdroplet formation, which affects the energy balance of the Earth. Figure 21 shows the change in the intensity of cosmic radiation modulated by the solar plasma, together with the change in the atmospheric coverage above the Earth's surface with clouds. Anomalies, i.e. deviations from the mean, for cosmic radiation that is absorbed by solar plasma and is further emitted by it, oscillate with a period of solar activity. The considered effect of cosmic rays on the atmosphere is associated with its ionization. It would seem that the energy spent on ionization is small, and this process cannot affect the energy of the atmosphere. Indeed, the rate of ionization of the atmosphere by cosmic rays per unit area of the Earth's surface is $4.5 \times 10^7 \text{ cm}^{-2} \text{ s}^{-1}$ [133], which corresponds to a total power of approximately $1 \times 10^9 \text{ W}$ [23] consumed on this process. This is eight orders of magnitude less than the power of solar radiation entering the atmosphere. Therefore, one would expect that cosmic radiation does not affect the atmospheric energy. Nevertheless, an action on the sensitive element of the chain of energy processes may require much lower power.

It follows from Fig. 21 that the correlation between the intensity of cosmic rays and the change in the area of clouds in the lower part of the atmosphere occurs in the 22nd solar activity cycle from 1981 to 1992. In the subsequent 23rd solar activity cycle, this correlation is absent. Apparently, this picture can be explained by the fact that cosmic rays significantly influenced the cloud growth in the 22nd solar cycle via the formation of condensation nuclei, whereas other channels then appeared to form the condensation nuclei of atmospheric water due to air pollution.

The presented analysis of Svendsmark et al. [134–137] made it possible to analyze the nature of the influence of cosmic radiation on the Earth's climate in the past and also became the basis of an experiment at the CERN accelerator, where the effect of cosmic radiation on atmospheric air was simulated by the action of synchrotron radiation. Although this concept of the influence of cosmic ray intensity on the Earth's climate causes discussions and objections, the very formulation of this problem shows that even low-energy processes in the atmosphere can affect its energy balance if they act on sensitive elements in the chain of energy processes.

Let us note one more aspect of the problem. Water condensation in the atmosphere begins with the formation of nanosize particles, whereas, focusing on thunder clouds, we deal with microdroplets, typical parameters of which are given by formula (6). This is due to the character of the water condensation in the atmosphere. Indeed, the formation and growth of the condensed water phase occurs mainly at altitudes of 2–5 km, where, due to the decrease in atmospheric temperature with altitude, the water vapor pressure becomes higher than the saturated vapor pressure due to penetration of jets of humid air from low layers of the atmosphere. In this region, an excess of water vapor is converted into a condensed phase, and, if condensation nuclei are present in the atmosphere in the form of ions and radicals, this process occurs during short times, less than 1 s.

During these times, an equilibrium is established between the gas and condensed water phases, and it is in areas containing small water drops, which are condensation nuclei, that the subsequent condensation of water vapor occurs if the jets of moist air penetrate the region of the location of small drops. At the same time, droplets grow in this region of the atmosphere as a result of coagulation, i.e., the merger of two drops at their collision. This process goes slower as a drop reaches a larger size and ends when the time it takes for a drop to leave the cloud becomes comparable to the time it grows. In this case, the drop reaches micron sizes. It should be noted that the time of drop growth or the time that water molecules stay in the atmosphere is 8–9 days, which is much longer than a typical time to establish equilibrium between the phases.

We add that, although the condensed phase of atmospheric water was considered to be microdroplets, i.e., it was considered liquid, for these processes it is not of principal. If this phase is solid (snow, ice, or their mixtures), the collision of two particles in different phase states leads to their charging and thus gives rise to atmospheric electricity [138]. This indicates the important role of condensation processes, not only for the formation of thermal radiation of the atmosphere but also for other atmospheric processes and phenomena.

4.4. Partial Atmospheric Emission

Let us consider the peculiarities of the formation of a flux of infrared radiation on the Earth’s surface. In accordance with the performed analysis, it is created by three components, molecules of water and carbon dioxide and also by water microdroplets. The absorption band of carbon dioxide molecules occupies the frequency range of 580–750 cm⁻¹ and is determined by three vibration transitions (Fig. 11). The absorption band of water molecules is in the range of 0–800 cm⁻¹ and overlaps with the range of absorption of carbon dioxide molecules. Thus, these molecules compete with the formation of thermal radiation from the atmosphere. The use of spectroscopic data from HITRAN bank facilitates the consideration of this competition with in the framework the line-by-line method, i.e., via the analysis of partial radiative fluxes of the atmosphere at each frequency. In this case, photons produced by each component are summed, and there is a total absorption coefficient (12) and a certain radiative temperature for each photon frequency (13).

Such a scheme makes it possible to separate the atmospheric radiation fluxes created by different components. In particular, the proportion of photons that reach the Earth’s surface and that originate from the emission of carbon dioxide molecules is k_{ω}/K_{ω} according to the formula (12). Table 2 contains the corresponding radiation fluxes due to each of the component, as well as the contribution of these components to the total radiation flux of the atmosphere.

At the present composition of the atmosphere, the total radiative flux of the atmosphere towards the Earth is fixed at 327 W/m². The same operation can be done for another content of the optically active components of the atmosphere with an account for that the total radiation flux is not fixed. The most common operation of this kind is to double the atmospheric concentration of carbon dioxide molecules, as proposed by Arrhenius in the end of 19th century [6]. The corresponding global temperature change ΔT is called the equilibrium climate sensitivity parameter (ECS) [139].

From Table 2 it follows that a doubling of the atmospheric concentration of carbon dioxide increases the flux due to carbon dioxide by about 6 W/m². In [20, 22] the value of 4 W/m² is given, which corresponds to the use of the spectrum-averaged absorption coefficient

Table 2. Radiation fluxes from the Earth’s atmosphere emitted by an indicated component and its portion (in brackets) of the total radiation flux, in W/m²

Component	CO ₂ molecules	H ₂ O molecules	Water microdrops
J_{\downarrow} , W/m ²	44(14%)	172(52%)	111(34%)
$J_{\downarrow}^{(2)}$, W/m ²	50(16%)	168(51%)	110(33%)

J_{\downarrow} corresponds to the modern atmospheric concentration of carbon dioxide, and the radiation flux $J_{\downarrow}^{(2)}$ relates to its double value.

of atmospheric water [113]. However, these values do not indicate an increase in the radiative flux to the Earth’s surface, since an increase in the radiative flux due to carbon dioxide molecules as a result of an increase in the atmospheric concentration of carbon dioxide is accompanied by a decrease in the radiation flux due to other components; this also follows from Table 2. The difference of radiation fluxes at a doubled and the contemporary atmospheric concentrations of CO₂ molecules, according to the considered line-to-line method, is

$$\Delta J = 0.7 \text{ W/m}^2. \tag{16}$$

Note that averaging the absorption coefficient of atmospheric water over frequencies gives for this value [122]

$$\Delta J = (1.0 \pm 0.2) \text{ W/m}^2. \tag{17}$$

One can understand the reason for the discrepancy of the above data. At frequencies with a large optical atmospheric thickness, the radiative temperature of the atmosphere T_{ω} is close to the temperature of the Earth’s surface, and the derivative of the partial radiative flux with respect to the number density of CO₂ molecules is relatively small. This means that the change in the radiative flux of the atmosphere to the Earth’s surface is determined by the frequencies at the boundary of the absorption band for carbon dioxide molecules. However, as follows from Fig. 18, water molecules predominate at the lower boundary of the carbon dioxide absorption band in the radiation of the atmosphere, while averaging of the absorption coefficient of water molecules over frequency eliminates this role.

When analyzing changes in the greenhouse effect as a result of changes in the concentration of CO₂ molecules as the optically active component of the atmosphere, we operate with the changes of radiative fluxes ΔJ to the Earth’s surface. It is clear that this will lead to a change in global temperature or the average temperature of the Earth. ΔT . The relationship between these parameters is expressed through the climate sensitivity parameter S , which is introduced by the relation [20, 39, 139, 140]

$$\Delta T = S\Delta J.$$

This parameter takes into account the feedback of the system with respect to external impact. That is, the additional radiative flux ΔJ aimed at the Earth's surface leads to an increase in its temperature, which creates energy fluxes which are proportional to temperature changes ΔT and compensate for this flow. In this case, the greatest uncertainty for the parameter S is due to water microdroplets. Indeed, an increase in the temperature of the Earth's surface changes the effective altitude at which water vapor condenses, which is amplified by large fluctuations in the course of this process. Note that, in the analysis of the radiation of a standard atmosphere, the radiation of the condensed phase of water was connected with the atmospheric energy balance, which eliminated this uncertainty. At the composition of the atmosphere, this condition is absent.

Thus, the error in the determination of the change in global temperature is much higher than the error in the change in radiation fluxes from the atmosphere as a result of changes in its composition. Along with the traditional means, the sensitivity of the atmosphere to changes in its composition by changes in the global temperature as a result of the doubling the carbon dioxide concentration [6], we note that a 10% increase in the atmospheric concentration of water molecules with account for radiative parameters of water microdroplets leads to an increase in radiative flux to the surface Earth's to about

$$\Delta J = 0.3 \text{ W/m}^2.$$

Let us return to the definition of the sensitivity parameter S . A thorough analysis [39] shows that, over a period of about a million years in the past, this parameter most likely varied from 0.6 to 1.2 W/m², which corresponds to a past change in global temperature of ECS = 0.4–0.8 K. For the modern atmosphere, the values obtained are closer to the lower limit. In particular, according to [122], $S = 0.42 \text{ W/m}^2$, which gives ECS = 0.3 K. Note that simpler models [23, 34] yield ECS = 0.4 ± 0.2 K, which is approximately 20% of the total temperature change according to (5). It can be seen that the contribution of the change in the carbon dioxide concentration to the change in global temperature is slightly higher than the contribution of carbon dioxide to the atmospheric radiation flux (Table 2).

It should be noted that the contribution of human activity to the transfer of carbon to the atmosphere does not exceed 5% (Fig. 6), from which it follows that the change in global temperature due to human industrial activity with doubling of the mass of atmospheric carbon dioxide gas to the atmosphere does not exceed 0.02 K. An increase in the atmospheric concentration of radicals and harmful impurities significantly affects the condensation processes in the atmosphere and thereby the parameters of atmosphere radiation. In addition, forest destruction changes the rate of the

photosynthesis process and thereby leads to an increase in the atmospheric concentration of carbon dioxide. As a part of the analysis, we can expect a significant impact of hydroelectric power plants on the increase in the planetary temperature, since the hydropower stations include large areas of open water.

As follows from the analysis, water droplets play an important role in atmospheric radiation. A simple model is used for drop radiation. It takes into account the strong interaction of drop molecules with an electromagnetic wave; for large drop sizes, the model of black body for infrared radiation holds true. It is interesting to compare the efficiency of interaction with radiation for a drop and for individual molecules, the absorption intensity of which is shown in Fig. 12. Take a drop with a radius $r_o = 10 \text{ }\mu\text{m}$, which is comparable to the wavelength of infrared radiation. According to formula (10), the absorption cross section for this drop is $3 \times 10^{-6} \text{ cm}^2$ within the black body model. The considered drop contains $(r_o/r_w)^3 = 1.4 \times 10^{14}$ molecules, where r_w is the Wigner–Zeits radius [141–143], which, in the case of water, is $r_w = 0.192 \text{ nm}$ [144]. Thus, the absorption cross section per molecule in this case is $2 \times 10^{-20} \text{ cm}^2$, whereas, according to Fig. 12, the maximum absorption cross-section of a water molecule in the center of the spectral line exceed 10^{-17} cm^2 . In this case, the absorption cross section of a free molecule averaged over the spectrum is estimated as $2 \times 10^{-19} \text{ cm}^2$ in this range of the spectrum.

4.5. Peculiarities of the Greenhouse Effect in the Atmosphere

The analysis made it possible to formulate a simple and strict scheme for the calculation of the atmospheric radiation fluxes in the infrared range of the spectrum. Below we summarize some results by presenting the peculiarities of this scheme and the character of the greenhouse effect of the atmosphere itself. Note the important role of the HITRAN database [8–10], which contains the parameters of the absorption coefficient (8) and (9) of molecular components in a convenient form and allows one to determine the absorption coefficient at each frequency directly. For a CO₂ molecule, this problem is simplified, since the absorption of IR radiation in this case is described by the regular model [145] due to the molecular symmetry. The number of vibration–rotation transitions that determine the radiative flux is restricted. Thus, the absorption band of CO₂ molecules extends from about 580 to 750 cm⁻¹, and, since the difference of neighboring frequencies is $4B = 1.56 \text{ cm}^{-1}$ ($B = 0.39 \text{ cm}^{-1}$ is the rotational constant of the carbon dioxide molecule), about 100 spectral lines give the main contribution to the radiative flux of atmospheric CO₂ molecules. Similarly, for the water molecule, approximately 50 spectral lines are used in the spectral range, in which the structure of the absorption band influences the

atmospheric radiative flux towards the Earth. All of this allows one on the basis of HITRAN data, to determine the gas absorption coefficient in a direct way with the line-by-line method.

Another peculiarity of the absorption spectrum of atmospheric air with optically active molecules is its oscillatory structure. For CO₂ molecules in atmospheric air, the ratio of the maximum absorption coefficient in the center of the spectral line to its minimum value between two lines in accordance with formula (11) is

$$\frac{k_{\max}}{k_{\min}} = \left(\frac{2\Delta\omega}{\pi\nu} \right)^2 = 44. \quad (18)$$

In the case of water molecules in atmospheric air, the oscillations are irregular and ratio (18) is much higher. With such a large amplitude of oscillations, the averaging of the absorption coefficient over frequencies can lead to noticeable errors.

Note that, according to Fig. 14, the boundary of the absorption band for the real absorption coefficient with oscillations is larger than for the average one. Thus, there are different values of radiative fluxes in these cases. Further, the averaging of the absorption coefficient of atmospheric water molecules leads to an increase in the change in the radiative flux of CO₂ molecules as a result of a doubling of their concentration in atmospheric air by 4 W/m² [13, 15, 113]. Taking into account the oscillations of the absorption coefficient of water molecules, we obtain a 1.5-fold higher value of this flux. Conversely, the change in the total radiative flux of the atmosphere is 1.5 times lower with allowance for oscillations than in the case of the absorption coefficient averaged over oscillations [formulas (16) and (17)].

Analysis showed that the frequency ranges, at which atmospheric molecules and microdroplets, are emitted are separated, with the interface between 750–780 cm⁻¹. The radiation of these components is also divided in a space, i.e., the main contribution to the molecular radiation follows from altitudes located below the clouds. In this case, we note that microdrops without impurities are transparent to radiation in the visible range of the spectrum, i.e., microdroplets can exist over areas with a transparent atmosphere for visible radiation. Further, with the contemporary composition of the atmosphere, about a third of the atmospheric radiative flux towards the Earth is formed by microdroplets. In this case, a change in global temperature causes a change in the radiative flux to the Earth's surface, due to a change in the total mass of water microdroplets in the atmosphere and a change in the lower edge of altitudes responsible for microdroplet emission. These altitudes are associated with the character of the condensation of atmospheric water; thus, analysis of the atmospheric processes with the participation of microdroplets allows one to convert more accurately the change in atmospheric radia-

tive flux due to a change in its composition to the change in global temperature.

Although our task is to develop an algorithm to calculate radiative fluxes to the Earth's surface due to changes in the concentration of greenhouse components, we will also analyze the results of such calculations, since our mass media spread false information. Leaving aside the question of whose interests they are serving, we will further present results that follow from this scheme. According to Fig. 7a, the rate of carbon dioxide accumulation in the atmosphere under current conditions corresponds to a doubling of the carbon dioxide concentration in the atmosphere after 120 years. Most of this accumulation is determined by the increase in global temperature in accordance with the concept of Pauling. The rest, about 20% of the growth is associated with the human mismanagement at the Earth, which is manifested, in particular, by the cutting and burning of forests and affects the photosynthesis rate at our planet. As for carbon dioxide emissions into the atmosphere as a result of the use of fossil fuels, since their contribution to the total carbon dioxide flux directed to the atmosphere is about 5% (Figure 6), the contribution of carbon dioxide emissions to the increase in global temperature is 1%. Note that the accuracy of the above theory corresponds to 10–15% for changes in radiative fluxes from the atmosphere to the Earth's surface and 40–50% for changes in global temperature due to an increase in greenhouse gas concentrations.

Note that the above results make it more realistic to evaluate various aspects of the contemporary energetics. In particular, it is believed that hydropower is clean, in contrast to thermal power plants, where energy is produced by burning fossil fuels, and this leads to the greenhouse effect due to the emission of carbon dioxide—a product of this process. However, the character of the operation of hydroelectric power plants also leads to an increase in the greenhouse effect, since hydroelectric stations must have reservoirs, and water evaporation from these reservoirs contributes to the greenhouse effect of the atmosphere. For definiteness, we will carry out the corresponding estimates for the Saratov hydroelectric power plant [146, 147], the power of which is 1.4×10^9 W, and the area of its reservoir is 1.8×10^3 km², as well as for the Volga hydroelectric power plant with the power of 2.7×10^9 W, where the reservoir area is 3.1×10^3 km² [148]. We assume that the average humidity before the construction of the reservoir corresponds to the standard atmosphere and is equal to 80% and that it is 100% above the reservoir. It was found above that a 20% increase in the atmospheric concentration of water causes an increase in the flux of atmospheric radiation by 0.6 W/m². Thus, due to the created reservoirs, the additional radiative flux to the Earth's surface is approximately 1×10^9 W for the Saratov power plant and 2×10^9 W for the Volga hydroelectric power plant. Thus, this power of the

Saratov power plant causes additional atmospheric radiative fluxes, and their powers are comparable with those of the power plants themselves.

In order to compare the efficiency of hydroelectric power plants and thermal power plants, we replace these hydroelectric stations with thermal stations that generate electrical energy when methane is burned. They release a specific energy per gram of carbon of 74 kJ/g [84]. We consider that a doubling of the flow of carbon dioxide molecules into the atmosphere leads to an increase in the radiative flux to the Earth's surface by 0.7 W/m². We obtain the corresponding increase in the power of thermal radiation to the Earth's surface due to additional fluxes of carbon dioxide into the atmosphere of 1.4×10^9 and 2.8×10^9 W in the case of the Saratov and Volga hydroelectric stations, respectively. As can be seen from the considered examples, the greenhouse effects due to hydro power plants and thermal power plants are comparable. Thus, the operation of hydroelectric power plants also causes the greenhouse effect, the power of radiation fluxes from the atmosphere to the Earth's surface are comparable, and the power transferred by these fluxes are comparable to the power of electrical energy generated at these power plants.

The result of the analysis is the creation of an algorithm to determine the radiative flux on the Earth's surface within the framework of the standard atmosphere model [5], i.e., an atmosphere with averaged parameters. This algorithm can be used to analyze the greenhouse effect for a metropolis with a size of at least several km, i.e., the size of the metropolis is much larger than the altitude at which the flow of infrared radiation to the Earth's surface. In this case, the parameters corresponding to this megacity, including the solar radiative flux, the vertical profile of the partial pressure of the components, and the atmospheric temperature should be entered into the presented algorithm. This approach allows one to fulfill the continuous monitoring of the infrared radiation of the atmosphere for a given megacity.

CONCLUSIONS

This article focuses on the energy balance of the atmosphere, rather than climate change. The climate problem (e.g., [149–154]) is much more complex and various than the considered problem of the greenhouse effect of the atmosphere. This allows the media to disseminate unreliable conclusions about the evolution of Earth's climate in the interests of European financial groups. Therefore, we briefly formulate the conclusions that follow from the scientific programs for the study of individual aspects of this problem, which were conducted mainly by NASA.

Note that global temperature changes can be recreated for the last 150 years or so, since the information used for this purpose comes from weather stations in different parts of the world, which were constructed in

the 19th century. Since that time, according to Fig. 3, the global temperature has increased by about 0.8 K [155], which is about 6% of the amplitude of the local temperature fluctuations over the last million years. Though there is no reliable possibility at the present level of atmospheric science to establish the cause of global warming, one can find in the past analogs of similar local temperature changes. It was in the 11th century, when warming was observed in northern Europe, that the Vikings occupied Greenland, and, according to its name, the surface of this continent was free of ice, which now covers it. In the 14th century, the Vikings left Greenland because of its cooling [156].

The analysis carried out in this paper is associated with atmospheric electricity and environmental problems of the atmosphere, for which the most important of the greenhouse components of the atmosphere are water microdrops and other aerosols [157, 158]. At the same time, atmospheric chemical impurities are the nuclei of aerosol condensation, and they are also captured by them, enhancing their growth. Therefore, the density of aerosols increases in a polluted atmosphere. Apparently, for this reason, the aerosol concentration in the Northern Hemisphere is about three times greater than that in the Southern Hemisphere [159].

In conclusion, we note that the presented algorithm to describe the greenhouse effect in the standard atmosphere can be used to monitor the greenhouse effect of individual megalopolises. For some of them, the atmospheric interaction with the oceans is important [160].

REFERENCES

1. Fourier, J.B.J., *Ann. Chim. Phys.*, 1824, vol. 27, p. 136.
2. Fourier, J.B.J., *Mem. Acad. R. Sci.*, 1827, vol. 7, p. 569.
3. Tyndall, J., *Philos. Mag. Ser.*, 1861, vol. 4, p. 146.
4. Tyndall, J., *Philos. Mag. Ser.*, 1863, vol. 4, p. 200.
5. *U.S. Standard Atmosphere*, Washington, DC: Gov. Printing Office, 1976.
6. Arrhenius, S., *Philos. Mag.*, 1896, vol. 41, p. 237.
7. Goody, R.M., *Atmospheric Radiation: Theoretical Basis*, London: Oxford Univ. Press, 1964.
8. Center for Astrophysics. www.cfa.harvard.edu.
9. HITRAN. www.hitran.iao.ru/home.
10. HITRAN Online. www.hitran.org/links.
11. Houghton, Y.G., *Physical Meteorology*, Cambridge: Cambridge Univ. Press, 1985.
12. Twomey, S., *Atmos. Environ., Part A*, 1991, vol. 25, p. 2435.
13. Smirnov, B.M., *Vvedenie v fiziku plazmy* (Introduction to Plasma Physics), Moscow: Nauka, 1975.
14. *Understanding Climate Change*, Washington, DC: U.S. National Acad. Sci., 1975.
15. Kiehl, J.T. and Trenberth, K.E., *Bull. Am. Meteorol. Soc.*, 1997, vol. 78, p. 197.
16. Smirnov, B.M., *Energetika atmosfery* (Energy of the Atmosphere), Moscow: Znanie, 1979, part 3.
17. Salby, M.L., *Fundamentals of Atmospheric Physics*, San Diego: Academic, 1996.

18. Seinfeld, J.H. and Pandis, S.N., *Atmospheric Chemistry and Physics*, New York: Wiley, 1998.
19. Seinfeld, J.H. and Pandis, S.N., *Atmospheric Chemistry and Physics*, Hoboken: Wiley, 2006.
20. Salby, M.L., *Physics of the Atmosphere and Climate*, Cambridge: Cambridge Univ. Press, 2012.
21. Lagzi, I., Mészáro, R., Gelybó, G., and Leelősy, Á., *Atmospheric Chemistry*, Budapest: Inst. Geogr. Earth Sci., 2013.
22. Hartmann, D.L., *Global Physical Climatology*, Amsterdam: Elsevier, 2016.
23. Smirnov, B.M., *Microphysics of Atmospheric Phenomena*, Ser.: *Springer Atmospheric Sciences*, Springer, 2017.
24. North, G.R. and Kwang-Yul Kim, *Energy, Balance, and Climate Models*, Weinheim: Wiley, 2017.
25. Solar Constant. <http://en.wikipedia.org/wiki/solar-constant>.
26. Foukal, P.V. and Lean, J., *Science*, 1990, vol. 247, p. 556.
27. Wilson, R.C. and Hudson, H.S., *Nature*, 1991, vol. 351, p. 42.
28. Fröhlich, C., *Space Sci. Rev.*, 2006, vol. 125, nos. 1–4, p. 53.
29. Mekaoui, S. and Dewitte, S., *Solar Phys.*, 2008, vol. 247, p. 203.
30. Fröhlich, C. and Lean, J., *Geophys. Rev. Lett.*, 1976, vol. 25, p. 4377.
31. Fröhlich, C. and Lean, J., *Astron. Astrophys. Rev.*, 2004, vol. 12, p. 273.
32. Kopp, G. and Lean, J., *Geophys. Rev. Lett.*, 2011, vol. 38, L01706.
33. Willson, R.C., *J. Geophys. Res.*, 1982, vol. 87, p. 4319.
34. Smirnov, B.M., *Europhys. Lett.*, 2016, vol. 114, p. 24005.
35. Hansen, J.E., Johnson, D., Lacis, A., et al., *Science*, 1981, vol. 213, p. 957.
36. Intergovernmental Panel on Climate Change, As the IPCC Finalizes its Next Big Climate-science Assessment, *Nature Looks at the Past and Future of the Planet's Watchdog*, *Nature*, 2013, vol. 501, p. 297.
37. Hansen, J., Sato, M., Ruedy, R., et al., <http://www.columbia.edu/jeh1/mailling/2016/20160120-Temperature2015>.
38. Smirnov, B.M., *Fizika global'noi atmosfery* (Physics of the Global Atmosphere), Dolgoprudnyi: Intellekt, 2017.
39. Palaeosens Project Members, Making sense of palaeoclimate sensitivity, *Nature*, 1913, vol. 91, p. 683.
40. Faure, G. and Mensing, D., *Isotopes: Principles and Applications*, Hoboken, NJ: Wiley, 2005.
41. Geochronology. <https://en.wikipedia.org/wiki/Geochronology>.
42. Faure, G., *Principles of Isotope Geology*, Cambridge: Cambridge Univ. Press, 1987.
43. Dickin, A.P., *Radiogenic Isotope Geology*, Cambridge: Cambridge Univ. Press, 1995.
44. Ruben, S., Kamen, M.D., and Hassid, W.Z., *Science*, 1939, vol. 90, p. 510.
45. Ruben, S. and Kamen, M.D., *Phys. Rev.*, 1940, vol. 5, no. 7, p. 549.
46. Ruben, S., Hassid, W.Z., and Kamen, M.D., *J. Am. Chem. Soc.*, 1940, vol. 62, p. 3443.
47. Petit, J.R., Jouzel, J., Raynaud, D., et al., *Nature*, 1991, vol. 399, p. 429.
48. CO₂ Proxy Data. www.co2.earth/21-co2-past.
49. Mekaoui, S. and Dewitte, S., *Solar Phys.*, 2008, vol. 247, p. 203.
50. Pedersen, T., Rosental, Y., Seitzinger, S., et al., *Science*, 2000, vol. 290, p. 291.
51. *The Carbon Cycle*, Wigley, T.M. and Schimmel, D.S., Eds., Cambridge: Cambridge Univ. Press, 2000.
52. Carbon Cycle. <https://en.wikipedia.org/wiki/Carbon-cycle>.
53. Hill, R., *Nature*, 1937, vol. 139, p. 881.
54. Hill, R., *Proc. R. Soc. London, Ser. B*, 1939, vol. 127, p. 192.
55. Jones, H.G., *Plants and Microclimate: A Quantitative Approach to Environmental Plant Physiology*, Cambridge: Cambridge Univ. Press, 1992.
56. Hall, D.O. and Rao, K.K., *Photosynthesis*, Cambridge: Cambridge Univ. Press, 1999.
57. Lawlor, D.W., *Photosynthesis*, Oxford: BIOS, 2001.
58. Rawsthorne, S., *Plant J.*, 1992, vol. 2, p. 267.
59. Blankenship, R.E., *Molecular Mechanisms of Photosynthesis*, London: Wiley, 2014.
60. Edwards, G.E. and Walker, D.A., *C₃, C₄: Mechanisms and Cellular and Environmental Regulation of Photosynthesis*, Oxford: Blackwell, 1983.
61. Ciesin. www.ciesin.org/docs/004-038/004-038a.html.
62. Greenhouse Effect. <https://en.wikipedia.org/wiki/Greenhouse-effect>.
63. Lean, J. and Rowntree, P.R., *J. Clim.*, 1997, vol. 10, p. 1216.
64. Hahmann, A.N. and Dickinson, R.E., *J. Clim.*, 2001, vol. 14, p. 1634.
65. Lawrence, D. and Vandecar, K., *Nat. Clim. Change*, 2015, vol. 5, p. 27.
66. www.ipcc.ch/publications-and-data/ar4/wg1/en/ch757-3.html.
67. Keeling, Ch.D., *Tellus*, 1960, vol. 12, p. 200.
68. Keeling, Ch.D., *Tellus*, 1976, vol. 28, p. 538.
69. Mauna Loa Observatory. <https://en.wikipedia.org/wiki/Mauna-Loa-Observatory>.
70. Earth System Research Laboratory, Global Monitoring Division. www.esrl.noaa.gov/gmd/ccgg/trends.
71. Lüthi, D., Le Floch, M., Bereiter, B., et al., *Nature*, 2008, vol. 453, p. 379.
72. Pauling, L., *General Chemistry*, San Francisco: Freeman, 1970.
73. Kauffman, J.M., *J. Sci. Explor.*, 2007, vol. 4, p. 723.
74. Calcium Carbonate. <https://en.wikipedia.org/wiki/Calcium-carbonate>.
75. Baumgartner, A. and Reichel, E., *The World Water Balance*, Amsterdam: Elsevier, 1975.
76. Peixoto, J.P. and Oort, A.H., *Physics of Climate*, Washington, DC: Am. Inst. Phys., 1992.
77. Trenberth, K.E., Smith, L., Qian, T., et al., *J. Hydro-meteorol.*, 2007, vol. 8, p. 758.
78. Water Cycle. <http://en.wikipedia.org/wiki/water-circle>.
79. Shiklomanov, I.A., in *Water in Crisis: A Guide to the World's Fresh Water Resources*, Gleick, P.H., Ed., Oxford: Oxford Univ. Press, 1993, p. 13.
80. Shiklomanov, I.A. and Rodda, J.C., *World Water Resources at the Beginning of the Twenty-First Century*, Cambridge: Cambridge Univ. Press, 2003.
81. Winter, T.C., Labaugh, J.W., and Franke, O.L., in *Water Budgets: Foundations for Effective Water-Re-*

- sources and Environmental Management, Reston, VA: U.S. Geol. Survey Circular, 2007, p. 1308.
82. Atmosphere of Earth. <http://en.wikipedia.org/wiki/Atmosphere-of-Earth>.
 83. USGS. <http://water.usgs.gov/edu/watercyrclatmo-sphere.html>.
 84. *Handbook of Chemistry and Physics*, Lide, D.R., Ed., London: CRC, 2003, 86th ed.
 85. Properties of Water. <http://en.wikipedia.org/wiki/Properties-of-water>.
 86. Green, H.L. and Lane, W.R., *Particulate Clouds: Dust, Smokes, and Mists*, Princeton: Van Nostrand, 1964.
 87. Fleagle, R.G. and Businger, J.A., *An Introduction to Atmospheric Physics*, San Diego: Academic, 1980.
 88. Reist, P.C., *Introduction to Aerosol Science*, New York: Macmillan, 1984.
 89. Salby, M.L., *Fundamentals of Atmospheric Physics*, San Diego: Academic, 1996.
 90. Hinds, W.C., *Aerosol Technology: Properties, Behavior, and Measurement of Airborne Particles*, New York: Wiley, 1999.
 91. Friedlander, K., *Smoke, Dust, and Haze: Fundamentals of Aerosol Dynamics*, Oxford: Oxford Univ. Press, 2000.
 92. Smirnov, B.M., *Phys.—Usp.*, 2014, vol. 57, no. 11, p. 1041.
 93. Mason, B.J., *The Physics of Clouds*, Oxford: Clarendon, 1971.
 94. Mason, B.J., *Clouds, Rain and Rainmaking*, London: Cambridge Univ. Press, 1975, 2nd ed.
 95. Leitch, W.R. and Isaak, G.A., *Atmos. Environ.*, 1991, vol. 25, p. 601.
 96. Liquid Water Content. <http://en.wikipedia.org/wiki/Liquid-water-content>.
 97. Kindel, B.C., Pilewskie, P., Schmidt, K.S., et al., *Atmos. Meas. Tech.*, 2015, vol. 8, p. 1147.
 98. Hurst, D.F., Oltmans, S.J., Vömer, H., et al., *J. Geophys. Res.*, 2011, vol. 116, D02306.
 99. Herzberg, G., *Molecular Spectra and Molecular Structure*, Princeton: Van Nostrand Reinhold, 1945.
 100. El'yashevich, M.A., *Molekulyarnaya spektroskopiya (Molecular Spectroscopy)*, Moscow: Fizmatgiz, 1963.
 101. Allen, H.C. and Cross, P.C., *Molecular Vib-Rotors: The Theory and Interpretation of High Resolution Infrared Spectra*, New York: Wiley, 1963.
 102. Landau, L.D. and Lifshits, E.M., *Kvantovaya mekhanika (Quantum Mechanics)*, Moscow: Nauka, 1974.
 103. Krainov, V.P., Reiss, H.R., and Smirnov, B.M., *Radiative Processes in Atomic Physics*, New York: Wiley, 1997.
 104. Khristenko, S.V., Maslov, A.I., and Shevelko, V.P., *Molecules and Their Spectroscopic Properties*, Berlin: Springer, 1998.
 105. Wien, W., *Wied. Ann. Phys. Chem*, 1896, vol. 58, p. 662.
 106. Reif, F., *Statistical and Thermal Physics*, Boston: McGraw Hill, 1965.
 107. Kondratyev, K.Ya., *Radiation in the Atmosphere*, New York: Academic, 1969.
 108. McCartney, E.J., *Absorption and Emission by Atmospheric Gases*, New York: Wiley, 1983.
 109. Liou, K.N., *An Introduction to Atmospheric Radiation*, Ser.: *International Geophysics*, vol. 84, Amsterdam: Academic, 2002.
 110. Petty, G.W., *A First Course in Atmospheric Radiation*, Madison, WI: Sunlog, 2006.
 111. Zdunkowski, W., Trautmann, T., and Bott, A., *Radiation in the Atmosphere*, Cambridge: Cambridge Univ. Press, 2007.
 112. Smirnov, B.M., *Fizika slaboionizovannogo gaza (Physics of Low-Ionized Gas)*, Moscow: Nauka, 1978.
 113. Smirnov, B.M., *Physics of Ionized Gases*, New York: Wiley, 2001.
 114. Electromagnetic Absorption by Water. <https://en.wikipedia.org/wiki/Electromagnetic-absorption-by-water>.
 115. Platt, C.M.R., *Q. J. R. Meteorol. Soc.*, 1976, vol. 102, p. 553.
 116. Whittaker, E.T. and Watson, G.N., *A Course of Modern Analysis*, London: Cambridge Univ. Press, 1940.
 117. Goody, R.M. and Yung, Y.L., *Principles of Atmospheric Physics and Chemistry*, New York: Oxford Univ. Press, 1995.
 118. Smirnov, B.M., *Plasma Processes and Plasma Kinetics*, Berlin: Wiley, 2007.
 119. Twomey, S., *Atmospheric Aerosols*, Amsterdam: Elsevier, 1977.
 120. Rozenberg, V.I., *Rasseyaniye i oslableniye elektromagnitnogo izlucheniya atmosferynymi chastitsami (Scattering and Attenuation of Electromagnetic Radiation by Atmospheric Particles)*, Leningrad: Gidrometeoizdat, 1986.
 121. Liou, K., *Radiation and Cloud Processes in the Atmosphere*, New York: Oxford Univ. Press, 1990.
 122. Smirnov, B.M., *J. Phys. D: Appl. Phys.*, 2018, vol. 51, 214014.
 123. Byers, H.R., *Elements of Cloud Physics*, Chicago: Univ. Chicago, 1965.
 124. Fletcher, N.H., *The Physics of Rainclouds*, London: Cambridge Univ. Press, 1969.
 125. Mason, B.J., *Clouds, Rain and Rainmaking*, Cambridge: Cambridge Univ. Press, 1975.
 126. Matveev, L.A., *Dinamika oblakov (Clouds Dynamics)*, Leningrad: Gidrometeoizdat, 1981.
 127. Pruppacher, H. and Klett, J., *Microphysics of Clouds and Precipitation*, London: Reidel, 1978.
 128. Young, K., *Microphysical Processes in Clouds*, New York: Oxford Univ. Press, 1993.
 129. Houze, R., *Cloud Dynamics*, San Diego: Academic, 1993.
 130. Mason, B.J., *The Physics of Clouds*, Oxford: Oxford Univ. Press, 2010.
 131. Boucher, O., *Atmospheric Aerosols: Properties and Climate Impacts*, Dordrecht: Springer, 2015.
 132. Ney, E.P., *Nature*, 1959, vol. 183, p. 451.
 133. Ruderman, M.A. and Chamberlain, J.W., *Planet. Space Sci.*, 1975, vol. 23, p. 247.
 134. Svensmark, H. and Friis-Christensen, E., *J. Atmos. Terr. Phys.*, 1997, vol. 59, p. 1225.
 135. Svensmark, H., *Proc. R. Soc. A*, 2007, vol. 463, p. 385.
 136. Svensmark, H., Bondo, T., and Svensmark, J., *Geophys. Rev. Lett.*, 2009, vol. 36, L151001.
 137. Svensmark, H., Englo, M.B., and Pedersen, J.O.P., *Phys. Lett. A*, 2013, vol. 377, p. 2343.
 138. Reynolds, S.E., Brook, M., and Gourley, M.F., *J. Meteorol.*, 1957, vol. 14, p. 426.
 139. Climate Sensitivity. <https://en.wikipedia.org/wiki/Climate-sensitivity>.

140. Cronin, T.M., *Paleoclimates: Understanding Climate Change Past and Present*, New York: Columbia Univ., 2010.
141. Bender, M.L., *Paleoclimate*, Princeton: Princeton Univ., 2013.
142. Wigner, E.P. and Seits, W.F., *Phys. Rev.*, 1934, vol. 46, p. 509.
143. Wigner, E.P., *Phys. Rev.*, 1934, vol. 46, p. 1002.
144. Smirnov, B.M., *Nanoclusters and Microparticles in Gases and Vapors*, Berlin: De Gruyter, 2012.
145. Elsasser, W.M., *Phys. Rev.*, 1938, vol. 54, p. 126.
146. Saratov Hydroelectric Station. https://en.wikipedia.org/wiki/Saratov_Hydroelectric_Station.
147. *Volzhskaya GES* (Volzhskaya Hydroelectric Power Station). <https://ru.wikipedia.org/wiki/Volzhskaya-GES>.
148. *Volgogradskoe vodokhranilishche* (Volgogradskoe Reservoir). https://ru.wikipedia.org/wiki/Volgogradskoe_vodokhranilishche.
149. Peixoto, J.P. and Oort, A.H., *Physics of Climate*, Washington, DC: Am. Inst. Phys., 1992.
150. Martyn, D., *Climates of the World*, Amsterdam: Elsevier, 1992.
151. Ruddiman, W.F., *Earth's Climate Past and Future*, New York: Freeman, 2000.
152. Weart, S.R., *The Discovery of Global Warming*, Harvard: Harvard Univ. Press, 2003.
153. Pierrehumbert, R.T., *Principles of Planetary Climate*, Cambridge: Cambridge Univ. Press, 2010.
154. Archer, D., *Global Warming: Understanding the Forecast*, New York: Wiley, 2012.
155. Global Climate Change, Vital Signs of the Planet. <http://climate.nasa.gov>.
156. Marsh, N. and Svensmark, H., *Space Sci. Rev.*, 2000, vol. 94, p. 215.
157. Ievlev, L.S., *Khimicheskii sostav i struktura aerizolei* (Chemical Composition and Structure of Aerosols), Leningrad: Leningrad. Gos. Univ., 1982.
158. Petryanov-Sokolov, I.V. and Sutugin, A.G., *Aerizoli* (Aerosols), Moscow: Nauka, 1989.
159. World Meteorological Organization. www.wmo.int/pages/themes/climate/causes-of-climate-change.php.
160. Gill, A., *Atmosphere—Ocean Dynamics*, San Diego: Academic, 1982.